Development of a Freeze-Drying Strategy to Store Human Bone Marrow Mesenchymal Stem/Stromal derived Extracellular Vesicles for Applications in Stroke

Brian Dorus

Thesis submitted to the University of Ottawa

in partial fulfillment of the requirements for the

Master's degree in Biomedical Engineering

Department of Chemical and Biological Engineering

Faculty of Engineering

University of Ottawa

ABSTRACT

Mesenchymal stem/stromal cells (MSCs) release Extracellular vesicles (EVs) that are believed to play a major role in nerve regeneration after stroke. However, a major complication when trying to transition MSC-EVs from a pre-clinical to clinical setting is the convenient long-term storage of MSC-EVs. Therefore, we developed a strategy to freeze dry MSC-EVs to store them for more practical clinical applications. We first determined the optimal trehalose concentration for freeze drying the MSC-EVs, and we subsequently investigated the optimal freezing conditions. It was determined that 100 mM of trehalose and freezing temperature at -20^{o}C were the optimal conditions to freeze dry the EVs. The therapeutic capabilities of the freeze-dried MSC-EVs was tested via tube formation assay and co-culturing them with neural stem/progenitor cells (NSPCs). It was found that human vein umbilical endothelial cells (HUVECs) treated with rehydrated MSC-EVs promoted tube formation suggesting the trophic factors in the MSC-EVs survived the freeze-drying process. As for the NSPC co-culture, all treatments involving rehydrated MSC-EVs protected by trehalose during the freeze-drying process promoted proliferation and did not affect their ability to differentiate into oligodendrocytes, astrocytes, or neurons. Determining the optimum freezing-drying conditions allows us to stockpile a large amount of MSC-EVs at room temperature for on-demand applications.

STATEMENT OF CONTRIBUTIONS

This thesis was written entirely by the author. Unless stated otherwise in the caption, all figures and tables were created by the author. All experiments were designed and analyzed by the author. The NanoSight experiments were performed by Jelica Mehic (Research Technician, stem cell – based therapeutics laboratory Regulatory Research Division, Center for Biologics Evaluation, BRDD, HPFB, Health Canada / Government of Canada). Neurosphere co-culture was performed by Charvi Syal (Research Technician, Ottawa Hospital Research Institute). The scientific guidance throughout the thesis were provided by Dr. Xudong Cao.

ACKOWNLEDGEMENTS

I would like to voice my appreciation to my supervisor Dr. Xudong Cao for providing me the chance to be part of this laboratory. I am profoundly thankful to him for his continuous leadership, counsel, and patience during my time at his laboratory.

I would like to thank everyone at the Stem Cell Based Therapeutics Laboratory at Health Canada, especially Dr. Jessie Lavoie. With her support throughout this journey I was able to achieve my full potential for development of this project.

I would also like to thank everyone at our laboratory for their assistance: Xingkai Hao, Yingshu Leng, Xiaotan Zhu, and Man Lu.

TABLE OF CONTENT

NOMENCLATURE, ABBREVIATIONS, SYMBOLS, GLOSSARY

AD	Adipose derived	MHC	Major histocompatibility complex
bFGF	Basic fibroblast growth factor	mEVs	Medium extracellular vesicles
BBB	Blood brain barrier	T_m	Melting temperature
BSCB	Blood spinal cord barrier	MSC	Mesenchymal stem cells
BDNF	Brain-derived neurotrophic factor	MPP	Metalloproteins
CCM	Cell conditioned media	miRNA	Micro Ribonucleic Acids
CNS	Central Nervous System	µm	micrometer
DC	Decompressive Craniectomy	MV	Microvesicles
DLL4	Delta like 4	MCAo	Middle cerebral artery occlusion
DF	Double filtered	MVB	Multivesicular bodies
ESCRT	Endosomal sorting complexes required for transport	NTA	Nano tracking analysis
H_D^0	Enthalpy	nm	nanometer
EGF	Epidermal growth factor	NF - B	Necrosis factor kappaB
EPO	Erythropoietin	NSPC	Neuronal stem/progenitor cells
ECM	Extracellular matrix	iNOS	Nitric oxide synthase
EV	Extracellular vesicles	NGS	Normal goat serum
FBS	Fetal bovine serum	PD	Parkinson disease
ΔG_D^0	Gibbs free energy	PBS	Phosphate buffer saline
T_g	Glass transition temperature	PDGF	Platelet derived growth factor
GFAP	Glial Fibrillary acidic protein	PVP	Polyvinylpyrrolidone
GvHD	Graft vs host disease	QbD	Quality-by-design
GF	Growth factors	RNA	Ribonucleic Acids
C_p	Heat capacity	SFM	Serum free media
HSC	Hematopoietic stem cells	sEVs	Small extracellular vesicles
HGF	Hepatocyte growth factor	SD	Standard deviation
hBM	Human bone marrow	SDF	Stromal derived factor
HDF	Human dermal factor	SGZ	Subgranular zone
HLA	Human leukocyte antigen	SVZ	Subventricular zone
HUVEC	Human umbilical vein endothelial cells	T	Temperature
HD	Hunting Disease	TSG	TNF-stimulated gene 6
IFN	Interferon	TEM	Transmission Electron microscopy
lEVs	Large extracellular vesicles	TNF	Tumour necrosis factor
LLPS	Liquid-liquid phase separation	VEGF	Vascular endothelial growth factor

LIST OF TABLES

LIST OF FIGURES

1 Introduction

1.1 Background

Mesenchymal stem/stromal cells (MSCs) have been demonstrated to have therapeutic capabilities that can be used for a wide range of diseases such as, stroke, spinal cord injury, lung injury, and kidney injury [1]. However, there are problems using MSCs in a clinical setting such as, abnormal karyotyping after multiple passages [2] and intravenous injected MSCs getting trapped in the lungs due to their large size [3]. Furthermore, pre-clinical studies have shown that the therapeutic mode of action for MSCs are the trophic factors they release, leading to research focusing on cell-free based therapies [4]. Among the factors released by MSCs, nano-scaled poly-dispersed particles, such as extracellular vesicles (EVs), have shown to retain the therapeutic capabilities of their parent MSCs [4]. However, MSC-EVs do have their own issues concerning mass production and storing them for long periods of time for their potential use in a clinical setting [5], [6]. Therefore, this thesis involves determining the optimum freeze-drying conditions for MSC-EVs by testing different freezing conditions and cryoprotectant concentrations, while investigating whether their therapeutic abilities are retained after two weeks of storage at room temperature.

Stroke is classified as a central nervous system (CNS) disorder that involves the abrupt death of brain cells due to the absence of oxygen and nutrients [7]. It can be categorized as two types: hemorrhagic where a blood vessel ruptures in the brain and ischemic where an artery is clogged due to a thrombus. It has become the second leading cause of death and third leading cause of disabilities worldwide [8]. Five million patients die from stroke while five million become permanently disabled [9] and in particular there are 878,500 survivors in Canada between the years of 2017-2018 [10]. Unfortunately, current treatment strategies can be ineffective and cannot completely reverse the neurological damaged sustained [11]–[13]. Some patients of an ischemic stroke can experience substantial brain swelling post stroke due to an increase in cerebral edema

leading to increased intracranial pressure, which is alleviated via a decompressive craniectomy (DC) procedure [14]–[16]. This operation requires removing a section of the skull, opening the dura, and placing a duraplasty over the opening to protect it from the environment while allowing the brain to expand [14]–[16]. In spite of being extremely invasive, the DC procedure reduces mortality rates but does not provide any therapeutic recovery to reverse the damage caused by the stroke [14], [17]. Thus, using an already characterized duraplasty, from a previous study [18], the end goal of this project is to produce a duraplasty that releases MSC-EVs that provide therapeutic recovery.

MSC-EVs are 50 to 200 nm spherical capsules that are released from MSCs that have similar therapeutic effects as their parent cells [19]. They have been shown to promote endogenous neurogenesis and angiogenesis, regulate the immune system, and repair brain matter [20]. The content within these MSC-EVs consist of proteins, lipids, microRNA (miRNA), mRNA, and non-coding RNA that can activate biological pathways contributing to functional recovery post stroke warranting their use [19]. Using MSC-EVs can bypass the need for cells and their affiliated problems such as, possible tumour formation, blockage of microvascular, or potential calcification [21]. However, a major issue when transitioning MSC-EV studies for clinical use is storing them for extended periods of time to stockpile enough MSC-EVs to treat an individual patient. Based off several clinical trials involving MSC-EVs, the working range for an effective dosage is $1x10^{10}$ to $6x10^{12}$ EVs [22], [23]. Then assuming a single cell can produce 1000 EVs, an estimated 100 to 1000M cells will be required to ascertain a single dose scheme within the working range [23], [24]. This will require significant large-scale production of MSC-EVs and updated preservation methodologies for possible clinical applications. However, there is a lack of concrete storage conditions for MSC-EVs requiring further inquiry into long term storage of MSC-EVs.

For short term storage EV solutions at kept at 4°C, nanoparticle analysis (NTA) shows that particle concentration starts to decrease after 48 hours of storage [25]. When suspended in polyphosphate-buffered saline (PBS) within polypropylene tube at 4°C the decrease in EVs range from 0.5 to 2.1 x 10^{10} particles/mL, where most of the loss is due to adsorption onto the tube walls [25]. While storing at lower temperatures such as, -20°C or -80°C, EV samples will undergo freeze-thaw cycles, which have shown to reduce EV particle and protein concentration after one cycle [26]. Therefore, a long-term storage method that can reduce particle and protein lose while being stored in an accessible manner is necessary. Freeze-drying EVs can preserve them for an extended period at room temperature but EV aggregation and protein loss can occur [27]. To circumvent this, a cryoprotectant such as trehalose is added to protect the EVs and its content during the lyophilization process [28]. However, there is a lack of knowledge for developing optimum freeze-drying conditions to ensure maximum MSC-EV recovery post rehydration. Current studies do not establish a working cryoprotectant concentration, nor freezing conditions for lyophilization resulting in inconsistent conditions being used throughout literature [27], [29]–[31]. Therefore, it is hypothesized that an optimal freeze-drying condition, in terms of cryoprotectant concentration and freezing conditions, can be achieved to preserve the bioactivity of MSC-EVs for use as a therapeutic drug to promote nerve regeneration post stroke.

1.2 Objectives

The goal of the thesis is to establish optimum freeze-drying conditions to stockpile a large amount of bioactive MSC-EVs at room temperature. To achieve this goal, the following objectives have been established:

1. Objective 1: MSC-EVs were frozen at -80°C in the presence of trehalose, a cryoprotectant, at concentrations of 0 mM, 50 mM, 100 mM or 200 mM to determine the optimum

trehalose concentration. Once rehydrated, these samples were then analyzed via nanosight, protein concentration, and structural integrity by transmission electron microscopy (TEM).

2. Objective 2: Once the optimum trehalose concentration was chosen, the second objective was to determine the best freezing conditions between -1°C/min, -20°C, -80°C, and -196°C (liquid nitrogen), in the presence of the optimum trehalose concentration, and the same quantitative/qualitative analysis was performed.
3. Objective 3: After the optimum freezing temperature and trehalose concentration were determine, the third objective was evaluating the bioactivity of the rehydrated MSC-EVs by performing a tube formation assay and co-culturing them with primary rodent neural stem/progenitor cells (NSPCs). Finally, we then ensured that the rehydrated MSC-EVs did not affect the differentiating potential of the NSPCs by immunostaining for oligodendrocytes, astrocytes, and neurons.

2 Literature Review

2.1 Central Nervous System (CNS)

The Central Nervous System (CNS) is made up of the brain and spinal cord. The brain is made of billions of nerves that send chemical and electrical signals to process sensory information, control blood pressure and breathing, and release hormones. While the spinal cord receives information from the senses and to send out orders to move muscles and control glands.

The CNS can be exposed to multiple diseases known as CNS disorders. These disorders can originate from biological entities or traumas that will affect the structure and function of the brain or spinal cord. Of all the disorders the CNS can be exposed to, this project focuses on stroke, which has shown to reduce motor, sensory, and cognitive function. Regretfully, the lack of self-regenerative capabilities within the CNS results in patients having very limited treatment options for stroke [32]. The brain is unable to regenerate post injury is because of the lack of endogenous

neurogenesis and damaged cells being replaced by scar tissue. While the absence of spontaneous regeneration within the spinal cord is due to no growth factors (GFs) or extracellular matrix (ECM) proteins that promote axon growth, the prevention of axonal growth due to inhibitor molecules, and glial scaring formation [33]. Current research for CNS disorder treatments focuses on delivering bioactive molecules for neuroprotection and endogenous neural stem/progenitor cells (NSPCs) proliferation and migration to the site of injury [34]. However, these treatment options are usually delivered orally or intravenously, which is impeded by the blood-brain barrier (BBB) and blood-spinal cord barrier (BSCB) [35].

The BBB/BSCB is a border of endothelial cells that only allow certain molecules to pass through into the CNS [36], [37]. Most preclinical studies deliver their treatments via orally or intravenously, but these barriers prevent the molecules from reaching the site of injury [35]. One method to overcome this obstacle is to increase the dosage and administration time but this can lead to toxicity [35]. To circumvent the BBB, treatments have been intraventricular injected into the brain but this approach is extremely invasive and can cause brain tissue damage due to the insertion of a catheter [38]. Therefore, current research strategies involve incorporating bioactive molecules into biomaterial for enhanced cellular proliferation and better drug concentration at the site of injury [11], [39].

2.2 Stroke

Stroke is the death of brain cells due to the lack of oxygen and nutrients, which can be categorized as hemorrhagic, bursting of a blood vessel, or ischemic, the blockage of a blood vessel [7]. The latter accounts for 87% of all strokes and 10% of these ischemic strokes can be classified as malignant due an increase in cerebral edema causing shifts in brain tissue and herniation, with a 78% mortality rate [7]. Symptoms of stroke include loss of sensation to one side of the body, fainting, confusion, dizziness, trouble speaking, and difficulty walking, while the severity of these

symptoms depend on the intensity of the stroke. Stroke is the second leading cause of death and third leading cause of disability globally [9], [40]; more specifically, of the 15 million people a year who experience a stroke, 5 million die and 5 million are permanently disabled [41]. Between 2017 to 2018 about 878,500 Canadians above the age of 20 had experienced a stroke, an increase of 16% over the last 5 years [10]. Unfortunately, the limited treatment options have left many stroke patients with disabilities for the rest of their lives [11]–[13].

2.3 Stroke Treatment Strategies

Post stroke therapies revolve around promoting circulation, returning blood flow of blocked vessels, and preventing death of ischemic cells. Administering intravenous thrombolysis 4.5 hours post stroke has shown to improve patient outcome but a limited number of patients re-establish flow in large vessels [42].

Current studies concentrate on inducing endogenous neurogenesis. After a stroke, neuronal progenitor stem cells (NPSCs) propagate in the subventricular zone and only a few migrate to the site of injury [43], [44], [45], [46]. Only 0.2% of NSPCs differentiate into mature neurons due to the lack of ECM and presence of cytotoxic factors, illustrating the self-regenerative deficiency of the CNS [47]–[50].

One of the earliest treatments researched for post stroke recovery is the exogenous administration of purified growth factors. For instance, basic fibroblast growth factor (bFGF) has shown to improve axonal growth near the focal infarct and can stimulate endogenous proliferation, migration to subventricular zone, and differentiation of NPSCs post administration [51]. Another growth factor of interest has been osteogenic protein – 1 (OP-1), as it can promote dendric outgrowth of neurons. Kawamata *et al*. had administered OP-1, via intracisternal, to MCAO stroked rats one and four days after stroke and observed strengthened sensorimotor recovery [52]. One of the more popular growth factors studied for stroke recovery is vascular endothelial growth

factor (VEGF) as it is shown to promote angiogenesis and has neuroprotective capabilities. Hayashi *et al*. had topically applied VEGF to MCAO stroked rats and observed smaller infarct volume, reduced BBB breakdown, and lower edema [53]. When Sun and colleagues had given MCAO stroked rats VEGF 3 days post induction, it reduced infarct volume, enhanced neurological recovery and survival of NPSCs in the subventricular zone [54]. An additional growth factor studied for stroke recovery is Erythropoietin (EPO), which has shown to promote sensorimotor recovery, increase the formation of microvessels around the infarct, and enhanced proliferation and differentiation of NPSCs in the subventricular zone [55]. Even though growth factors are able to pass the BBB, as it is broken open post stroke, and promote functional recovery, *in vivo*, a complication that arises when trying to translating to a clinical setting is the presence of proteases in the blood stream reducing their potential potency [56]. This has led researchers towards a cellular based therapy for stroke recovery.

NSPCs are multipotent primary cells that can differentiate into mature cell lineages, such as astrocytes, oligodendrocytes, and neurons both *in vivo* and *in vitro*. The use of stem cells, in particular mesenchymal stem/stromal cells (MSCs), have shown to promote proliferation and migration of NSPCs with *in vivo* animal stroke models [57]–[64]. The trophic factors released from MSCs is the driving force that promotes endogenous neurogenesis. They release soluble proteins such as VEGF [65], hepatocyte growth factor (HGF) [66], Wnt-5a/b [65], and platelet derived growth factor (PDGF) [67]. The most important factor released from MSCs are extracellular vesicles (EVs) as this cargo contains similar soluble proteins and nucleotides that can promote functional recovery post stroke.

2.3.1 Decompressive Craniectomy

Stroke can cause large swelling due to increased cerebral edema leading to damaging the encompassing brain tissue. A surgical procedure is often required as medication cannot supress

the increased intracranial pressure. Therefore, a DC is performed to release the stress exerted on the brain. The two types of patients that receives a DC procedure are: (1) patients that experienced a malignant middle cerebral artery infarction; (2) patients with large cerebral infarction [42]. Of the ischemic strokes that occur every year, only 0.3% are qualified for the DC procedure [68].

DC relieves intracranial pressure by removing a part of the skull and opening the dura [14]–[16]. Then to protect the brain from the environment, a duraplasty material is placed over the opening [16]. Even with the extreme invasiveness of this procedure, there are studies showing significant reduction in patient mortality [16], [69], [70]. However, DC does not improve the already lost brain function caused by the initial stroke onset [14], [17]. Furthermore, commercially available duraplasties do not provide any therapeutic benefits. Therefore, the overall goal of this project is to incorporate MSC-EVs into a biocellulose based durplasty, our research group had previously developed, for direct delivery of a therapeutic to the site of injury [18].

2.4 Mesenchymal Stem/Stromal Cells

First discovered in 1970, Friedenstein *et al*. isolated the content from the bone marrow and spleen of guinea-pigs and were described as monolayer forming fibroblastoid cells [71]. These cells displayed the ability to self-renew, differentiate into osteocytes, and play a vital role in hematopoiesis [71]. T.M Dexter *et al*. had demonstrated that hematopoiesis and maintenance of hematopoietic stem cells (HSCs) is greatly influenced by an adherent layer of MSCs [72]. They are known for their multilineage differentiation into osteocytes, adipocytes, and chondrocytes, and their ability to regenerate *in vitro*, but have a restricted lifespan [73], [74]. Furthermore, *in vitro* cultured MSCs have shown to promote angiogenesis, prevent apoptosis and inflammation, and modulate the immune system via a paracrine and contact-dependent manner [75]. A key ability MSCs possess is their immune advantage that prevents allogenic reactions due to their low amount of MHC class I and HLA I, and absence of MHC II and HLA-DR [76]. As a result, transplanting

MSCs into humans will not cause an allogeneic reaction due to this histo-incompatibility [76]. Their therapeutic capabilities can be attributed to their ability to home to locations of injury due to chemokine receptors expressed on their membrane and/or their aptitude to release regulatory proteins and bioactive factors at the site of injury [76].

2.5 Paracrine Mode of Action of MSCs

The theory of MSCs using a paracrine mode of action was first speculated when preclinical studies had shown that similar therapeutic effects can be observed between MSC-conditioned media (MSC-CCM) and MSCs. This theory was then reinforced by observing an improvement in myocardial infarction within mice when MSCs were intravenously administered [77, p. 6], [78]. They found that a majority of the transplanted MSCs were trapped in the lungs and concluded that the paracrine factors released by the cells had a therapeutic effect on the infarction [77, p. 6], [78]. In fact a few studies believe that the MSC regenerative capabilities are driven by trophic factors alone rather than a cellular manner [4]. The secretomes released by MSCs include soluble proteins, microvesicles, and/or extracellular vesicles (EVs) [4]. These finding have prompted several studies to focus on MSC-EVs being a potential therapy over their cellular counterpart. Even though MSCs have shown a lot of promise as a potential treatment for several diseases, cell-based therapies have problems of their own. Some challenges that occurred while using cells is their tumorigenic potential, obstructing microvasculature, and potential of calcification [21]. EVs can avoid tumour formation as they do not contain nuclei and due to their small size they cannot occlude microvasculature [21]. Additionally, the membrane of MSC-EVs are similar to the cells they derive from, thereby inheriting the immune privilege MSCs have [79]. Altogether, developing therapies centered around MSC-EVs could lead to cheaper and more effective treatment offers for diseases with limited options.

2.6 MSC Derived Extracellular Vesicles

EVs isolated from MSCs have shown to enhance a wide array of therapeutic mechanisms via a protein-based mode of action, suggesting that MSC-EVs can substitute their parent cells as a potential treatment [21]. MSC-EVs have shown to treat a multitude of diseases associated with the kidney, heart, brain, and lungs [80]–[93]. The surface markers and signalling molecules found in MSC-EVs can also be found on their parent cells hence possibly imitating the therapeutic capabilities of MSCs [94]. The different types of cargo detected in MSC-EVs have reported to decrease oxidative stress, encourage angiogenesis, and control neurite growth both *in vitro* and *in vivo* for cardiovascular disease and ischemic stroke [95]. Due to these findings clinical trials to develop a MSC-EV based treatment for graft vs host disease (GvHD), chronic kidney disease, type I diabetes Mellitus, and ischemic stroke have started [96].

2.7 Extracellular Vesicles – Overview

It was only recently that EVs have been identified as a major player in cell-to-cell communication and before that there were thought to be a mechanism for cellular waste disposal [97]. Johnstone *et al*. first discovered EVs while studying the maturation of reticulocytes to erythrocytes [98]. He called them "exosomes" because he noticed their production is analogous to reverse endocytosis, where internal vesicular components are released rather external components internalized into the cell [99]. EVs can be detected in all bodily fluids and released from almost all cell types as they maintain tissue homeostasis and play a key role in pathological diseases allowing them to act as biomarkers [100]. Due to their ability to mimic the therapeutic capabilities of their parent cells, the interest in EVs for medical purposes has grown exponentially [101]. They have the ability to be internalized into cells (via endocytosis) or fuse with their membrane to deliver bioactive molecules involved in cell-to-cell communication or transfer surface receptors/lipids [102]. In addition transferring molecules, EVs can act as a ligand to stimulate signalling pathways [102].

According to the International Society of Extracellular Vesicles (ISEV), EVs can be categorized based on their sizes. Small EVs (sEVs) have a diameter less than 200 nm and medium/large EVs (m/lEVs) have a diameter greater than 200 nm [103]. However, most cells produce a heterogenous population of EVs due to the different biogenesis pathways involved in their production.

2.8 Biogenesis of Extracellular Vesicles

Before the ISEV established characteristic parameters for EVs, they were categorized as exosomes (30 – 180 nm), microvesicles (100 – 1000 nm), and apoptotic bodies (1 to 5 mm) [19]. Exosomes are synthesized by late endosomes, which form by inward budding of the multivesicular body (MVB) membrane [19]. Within the MVB the late endosome membrane is turned inside out forming exosomes, in which proteins are integrated into the invaginated membrane and the cytosol is engulfed by the exosomes containing proteins, lipids, mRNA, and microRNA [19]. The MVB then travels to the plasma membrane and once it fuses with the membrane the exosomes are released into the extracellular space [19]. On the other hand, the MVB can be sent to lysosomes for degradation [19]. Exosomes are a biconcave or cup-like shape when prepared by artificial drying, and are spherical in shape when in solution[104], [105]. Studies have reported that a family of proteins known as endosomal sorting complex required for transport (ESCRT) work together to control MVB formation, vesicle budding, and protein sorting [104], [105]. The ESCRT mechanism begins by the ubiquitination of proteins associated with the endosomal membrane via the ubiquitin-binding subunits found on ESCRT-0 [104], [105]. After initiation, ESCRT-I and ESCRT-II form a complex with ESCRT-III that stimulate the budding process [104], [105]. Once the buds are cleaved to form exosomes, ESCRT-III dissociates from the MVB as it travels to the plasma membrane to release the exosomes via exocytosis or to lysosomes for destruction [104], [105]. Figure 1 is a simplified depiction of the production of EVs.

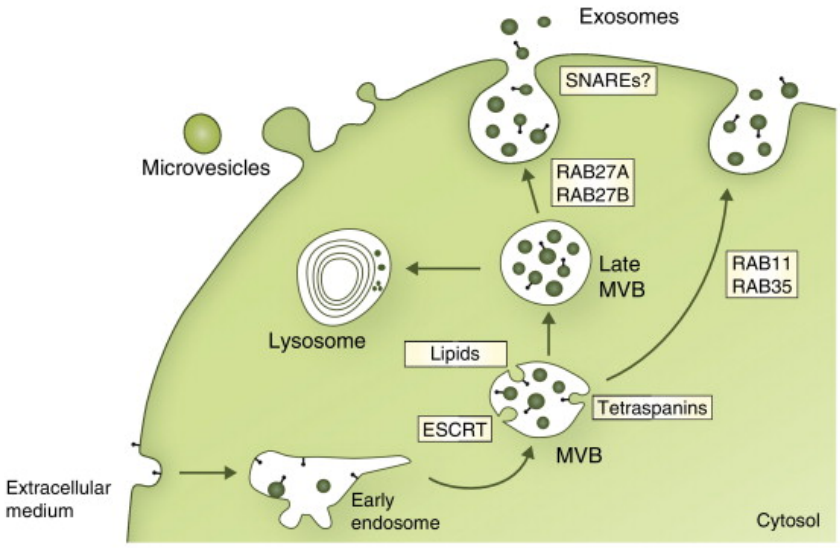

Figure 1. Biogenesis of exosomes and microvesicles from production to release. Reprinted from Current opinion in cell biology, Vol: 29, Joanna Kowal, Mercedes Tkach, Clotilde Thery, Biogenesis and secretion of exosomes, pg. 10, 2014, with permission from Elsevier [106].

MVs are heterogenous membrane vesicles synthesized by outward budding of the plasma membrane [104], [105]. While apoptotic bodies are formed at the final stages of apoptosis and contain organelles, membranes, and cytosol content [104], [105]. Of the three types of EVs, exosomes are studied the most as their small size and therapeutic capabilities give them the potential to become a treatment for several diseases.

2.9 Therapeutic Abilities of MSC Extracellular Vesicles

From multiple preclinical and clinical studies, MSCs have shown to promote endogenous neurogenesis, angiogenesis, and immunomodulation post stroke for functional repair. The therapeutic mode of action of MSCs was believed to be cellular replacement at the site of injury once they are administered *in vivo* [107]. However, several reports have indicated that a majority of the MSCs are trapped in the lungs preventing their travel to the site of injury and replace damaged brain cells but post stroke recovery was still observed *in vivo* [108]. This recovery was primarily driven by the release of trophic factors from the exogenous MSCs that enhance endogenous recovery mechanisms [109]. Of the factors released from MSCs, EVs are being

researched the most due to having similar therapeutic capabilities as their parent cells as their cargo containing proteins, lipids, microRNA, mRNA, and non-coding RNA.

2.9.1 Neuroprotective Capabilities of MSC-EVs

Neurogenesis is a biological process that promotes the formation of neurons. The subventricular zone (SVZ) and subgranular zone (SGZ) of the brain is where neurogenesis occurs [110, p. 3], [111]–[113]. Stem cell therapy improves functionalities post stoke by forming new NSPCs that migrate to the site of injury and differentiate. As mentioned beforehand, several *in vivo* studies have reported that transplanted stem cells promote proliferation and migration of NSPCs via trophic factors due to being trapped in the lungs instead of cellular replacement [108]. For instance, a study involving hypoxia conditioned human bone marrow derived MSCs (hBM-MSCs), MSCs cultured in 0.5% O_2, has shown to increase the expression of proteins involved in stroke recovery such as, brain-derived neurotrophic factor (BDNF), vascular endothelial growth factor (VEGF), erythropoietin (EPO), stromal derived factor-1 (SDF-1) [57], [114]. In addition to soluble factors, recent reports have indicated that EVs released from transplanted MSCs play a vital role in promoting endogenous neurogenesis for post stroke recovery. For example, Doeppner *et al*. had treated MCAO stroked mice with MSCs or MSC-EVs, and observed a significant increase in neural density at the ischemic region for both treatments but did not report a significant difference between the two treatments [58]. Another study comparing the treatment of stroked rats with MSCs and their MSC-EV showed that both treatments had a similar increase in the number of immature progenitor neurons in the ipsilateral and contralateral hemisphere [59]. These comparison studies have led to solely using MSC-EVs as a potential cell-free based therapy.

One of the mechanisms used by MSC-EVs are proteins that promote endogenous neurogenesis such as, BDNF, VEGF, and platelet derived growth factors (PDGF). Chen *et al*. had treated MSCs with prostaglandin E2 receptor 4 (EP4) resulting in high levels of both VEGF and BDNF in MSC-

EV cargo [60]. While Yuan *et al*. had shown that hBM-MSC-EVs are abundant in fibronectin, which is known to regulate substances that enter the brain, control receptor activation, and exert neuroprotective roles [61]. In addition to proteins, numerous reports have found the MSC-EVs can transfer miRNA into brain cells to enhance stroke recovery. Administering MSC-EVs to mice subjected to photothrombosis resulted in cortical neural progenitors migrating to the site of injury and gaining neuronal identity due to the transfer of miR-124 [62]. Another instance of miRNA transfer is when a study reported that MCAO stroke induced rats treated with BM-MSCs had increased levels of Ki-67 and DCX, markers involved in cellular proliferation and neuronal migration respectively, due to transfer of miR-184 [59]. Xin *et al*. had treated stroked rats with MSC-EVs leading to the transfer of miR-133b to astrocytes and neurons resulting in elevated neurite branch length and number [63]. In another study performed by Xin *et al*. they observed the transfer of miR cluster 17-92 from MSC-EVs to brain cells of stroked rats leading to the inhibition of phosphatase and tensin to activate the rapamycin/glycogen synthase kinase 3β signalling pathway resulting in enhanced neural plasticity [64]. With NSPCs proliferating, migrating, and differentiating into mature neurons, they need a source of nutrients and oxygen from blood vessels. However, a stroke causes all surrounding blood vessels to be damaged requiring a new network of vessels to be formed via angiogenesis.

2.9.2 Angiogenic Potential of MSC-EVs

For successful stroke recovery both angiogenesis and neurogenesis need to be activated to ensure proper brain remodeling. Both mechanisms work together by supplying nutrients and oxygen to the cerebral injury leading to the migration of neuroblasts that will differentiate into adult brain cells [115], [116]. As these neuroblasts migrate, they will release trophic factors that will induce the branching of blood vessels from pre-existing ones [115], [116]. In a similar fashion to neurogenesis, trophic factors released by stem cells are a major part of the mechanism utilized by

MSCs, which are delivered by EVs. Another study performed by Doeppner *et* al. has shown that treating stroked rats with either MSCs or MSC-EVs increased the number of endothelial cells in the ischemic striatum to a similar extent [58]. Studies had identified angiogenic proteins such as, VEGF, hepatocyte growth factor (HGF), PDGF, and Ang-1 loaded in MSC-EVs, which has shown to increase the number of endothelial cells in the ischemic boundary zone of stroked rats [59], [117], [118]. H. Gonzalez-King *et al*. had identified the transmembrane protein, jagged1, in human MSC-EVs leading to the activation of the notch signalling pathway in endothelial cells resulting in their growth and proliferation *in vitro* [119]. In addition to angiogenic proteins, MSC-EVs contain miRNA that influence angiogenesis such as, miR-181b which has shown to promote migration and proliferation of brain microvascular endothelial cells *in vitro* [120]. Zhang *et al*. had loaded miR-210 into MSC-EVs to transfer into brain cells, which have shown to reduce caspase activity to impede apoptosis all while upregulating the expression of VEGF [121]. D.R Cooper *et al*. isolated EVs from adipose derived MSCs (AD-MSCs) and performed a scratch assay with human dermal fibroblasts (HDF) showing that AD-MSC-EVs promote cell migration and angiogenesis for ischemic wound healing due to the long noncoding RNA (lncRNA) MALAT [122]. While M.Ging *et al*., had demonstrated that MSC-EVs can transfer the pro-angiogenic microRNA, miR-30b to human umbilical vein endothelial cells (HUVECs) leading to an increase in tube-like structure formation *in vitro* [123]. Another study had shown that AD-MSC-EVs can transfer miR-125a to endothelial cells leading to the repression of angiogenic inhibitor delta-like 4 (DLL4) and an increase in endothelial cell proliferation [124]. Even with endogenous neurogenesis and angiogenesis mechanisms active to repair the damage caused by stroke, the immune system induces continuous damage due to its inflammatory response that needs to be controlled.

2.9.3 MSC-EVs and Immunomodulation

Prolonged post stroke damage is well documented due to the immune system activating inflammatory mechanisms that damage intact brain cells [125]–[127]. The inflammatory response post stroke can be categorized as followed, activation of microglial cells, destruction of the blood brain barrier (BBB), intrusion of external immune cells and their release of inflammatory cytokines [125]–[127]. MSC-EVs treatment post stroke involves regulating their inflammatory responses.

The most common macrophage located in the brain are microglial cells that activate rapidly post stroke [128], [129]. Microglial can take two forms: In the M1 configuration microglial cells destroy foreign entities and release cytokines. While in the M2 form, microglial will promote wound healing and tissue repair [128]. Regrettably, after a stroke M1 microglial is activated as the immune system believes that the dead cells and its content are foreign. Brain damage is further intensified, as the M1 microglial release pro inflammatory cytokines like interleukin-1 β, interleukin-6, tumour necrosis factor α (TNF- α), and interferon-γ (IFN-γ) [127], [130]. One method that has shown to shift the polarization of microglial from M1 to M2 is treating stroked rats with adipose derived MSC-EVs (AD-MSC-EVs) due to their cargo containing miR-30d-5p [131]. Another instance of microglial shifting towards the M2 phenotype was a report that intravenously administered a stroked rhesus monkey with MSC-EVs resulting in reduced neuroinflammation [132].

In addition to M1 microglial activation, stroke causes serious damage to the BBB leading to an imbalance in homeostasis of the cerebral microenvironment. Once the BBB is destroyed, circulating cytokines and inflammatory cells can now enter the brain to cause further damage [133], [134]. The damage done to the BBB is brought by metalloproteins (MPPs) that breakdown tight junction proteins, which are crucial for barrier formation and maintaining BBB integrity [127], [135]. To attenuate BBB damage, one study has shown that transplanted MSCs can release

soluble factors such as, TSG-6, that block the NF-κB signalling pathway reducing the activity of MMPs [136], [137]. Kalani *et al*. had shown that treating stroked rats with stem cell EVs lead to an increase in expression of tight junction proteins, claudin-5 and occludin [138].

With the BBB unable to stop circulating compounds from entering the brain, peripheral immune cells can invade the brain causing secondary injury to the brain [135], [139], [140]. First, neutrophils infiltrate the brain causing post stroke damage by releasing MMPs and nitric oxide synthase (iNOS) [141]. In the later stages of stroke lymphocytes enter the brain parenchyma and release pro-inflammatory cytokines such as, (IFN-γ) and interleukin-17 [142]–[144]. To attenuate infiltrating immune cells, Webb *et al*. had treated a stroke pig model with stem cell EVs resulting in an increase of regulatory T cells in the brain, which are cells that supress pro-inflammatory responses [145]. While Dabrowska *et al*. had intravenously administered a stroked rats with MSC-EVs resulting in a decrease of immune cells such as, $CD45^+$ leukocytes and $CD8^+$ T cells [146]. Even though MSC-EVs provide multiple therapeutic benefits for a potential stroke treatment, there are still limitations on using MSC-EVs.

2.10 Storage Methods for Extracellular Vesicles

Even though MSC-EV are a promising tool for cell-free based stroke therapy, many complications arise when trying to transition the therapy to a clinical setting. In particular, the preservation of EVs to maintain their biological activity and to ensure enough are available to treat an individual patient. Therefore, different storage methods have been investigated for long term storage of EVs, which include cryopreservation and lyophilization.

2.11 Cryopreservation of Extracellular Vesicles

Storing biological samples at temperatures low enough, such as 4^{o}C, -80^{o}C, and -196^{o}C, to reduce biochemical reactions and to retain functional stability is known as cryopreservation. However, storing EVs with this method have shown to denature proteins, reduce protein content, reduce

particle concentration, and reduce biological activity. For example, storing EVs at 4°C for 48 hours in polypropylene tubes resulted in an EV particle loss of 51 ± 3% primarily due to adsorption of vesicles onto the tube walls [25]. Using low protein binding tubes can reduce particle loss ton 33% but this is still substantial [25]. Therefore, freezing EV samples has been investigated, which has its own problems including protein denaturing, drastic change in solute concentrations, and damages caused by ice formation all leading to reduced protein content and EV count [147].

2.11.1 Cold Denaturing

The unfolding of proteins is directly related to Gibbs free energy and the thermodynamically stability of the protein [148]. The Gibbs free energy (ΔG_D^0) can then be quantified by the following equation [148].

$$\Delta G_D^0 = \Delta H_D^0 \left(1 - \frac{T}{T_m}\right) + \Delta C_p \left[(T - T_m) - Tln\left(\frac{T}{T_m}\right)\right] \quad (1)$$

Where T_m is the midpoint of the unfolding transition, ΔH_D^0 the change in enthalpy between the folded and denatured protein, and ΔC_p is the change in heat capacity between the folded and denatured protein. It is well known that increasing the temperature denatures proteins, represented by a negative ΔG_D^0 [148], [149]. Another instance of negative ΔG_D^0 is when the change in heat capacity of denatured proteins is a large positive number, which occurs when the temperature drops below 0°C. In terms of determining the mechanism for cold denaturing, it is believed that at cold temperatures the hydrophobic residue groups become soluble in the aqueous solution [148]–[150]. To counter act cold denaturing a cryoprotectant is usually added and results suggest a reduction in the rate of protein denaturing due to decreasing protein mobility and the hydrogen bonds it forms with the proteins.

2.11.2 Freeze – Concentration

When a sample is being cooled the entire solution is not frozen instantly causing the formation of an ice-water interface. Since the freezing of all the water in a solution is not instant the concentration of solutes in the liquid fraction of the solution start to increase. Then as ice crystallization continues the concentration and viscosity of the liquid fraction continues to increase, which has been shown to increase the rate of biomolecular degradation, cause drastic changes in pH, and promote liquid-liquid phase separation [147].

2.11.2.1 Protein Degradation and Membrane rupturing due to an Increased Solute Concentration

While a biological sample is being frozen the unfrozen fraction can experience severe changes in solution concentration and viscosity that can reach up to seven orders in magnitude greater than the starting solution [151]. Samples containing proteins or liposomes would encounter a tremendous increase in concentration and viscosity leading to an increase in bimolecular degradation reactions [151]. It was assumed that the decrease in temperature would oppose this reaction but the combination of both high concentration and viscosity pushes the degradation forward [151]. Generally, there is expected to be partial coupling of degradation rate to viscosity and therefore reaction rates should be increased between 1 and 2 orders of magnitude [151]. Multiple publications have recorded evidence of ionic and enzyme-catalyzed reactions during freezing [152]–[157].

Furthermore, the increase in solute concentration creates an osmotic gradient across the lipid membrane causing osmotic shock. This gradient can either shrink or swell liposomes and EVs causing their membrane to rupture and leak. Along with degrading proteins and osmotic shock, the drastic change in solute concentration will cause a shift in pH [152]–[157].

2.11.2.2 Change in pH due to Crystallization of Solutes

Phosphate buffer systems have been shown to experience significant changes in pH (3 to 4 pH units) as the concentration of solutes, such as sodium and potassium, start to increase when phosphate buffer saline (PBS) begin to form ice crystals [158]–[161]. The change in pH is dependent on the type of salt present, the initial solute concentrations, and freezing protocol (ice seeding or no seeding). In the case of sodium PBS systems, the Na_2HPO_4 is less soluble than NaH_2PO_4, resulting in its precipitation when freezing leading to a decrease in pH of approximately 3 pH units [161]. As for potassium PBS systems, KH_2PO_4 precipitates out of solution instead of the dibasic salt, K_2HPO_4, leading to a more alkaline solution [161]. The presence of other solutes, like NaCl, increase the ionic product of the of the precipitated dibasic salt intensifying the pH shift. Proteins stored in an acidic or alkaline solution can disrupt hydrogen bonding throughout the protein structure leading to unfolding and reducing biological activity. As for EVs, Cheng et al. has reported that storing EVs isolated from HEK 293T cells in either an acidic (pH 4) or basic (pH 10) solution lead to a significant decrease in particle concentration when compared to samples stored in a neutral solution (pH 7) [162]. In order to mitigate solute crystallization, a stabilizer is introduced to keep the pH neutral while freezing [158], [163], [164].

2.11.2.3 Liquid-liquid phase separation

As the temperature decreases, the increase of solute concentration can lead to liquid-liquid phase separation (LLPS) in the liquid fraction [165]. LLPS is a phenomenon where a liquid solution separates into two liquid phases where each phase has different solute concentrations [165]. This occurrence has been reported in protein: protein, protein: electrolyte, and protein: sugar mixtures [166]–[168]. The phenomenon of LLPS can lead to some EVs not being protected by any stabilizer in one of the phases, different solute concentrations in different phases can lead to a different pH

in each phase, and if one phase has a higher EV concentration then aggregation can occur [169]. To mitigate these problems reports have suggested to introduce a cryoprotectant that will increase the T_g of the solution or to control process variables such as the cooling rate [169].

2.11.3 Ice-Water Interface

Ice formation is the primary reason why biological samples experience the stress mentioned above and is heavily related to freezing rates. Since the entire solution does not freeze instantly, an ice-water interface forms leading to proteins and liposomes being adsorbed at the interface resulting in their deformation[170], [171]. Rapid freezing has shown to generate a large ice-water interface while the opposite was observed for slow freezing solution [147]. One report demonstrated that rapid quenching resulted in all 6 of their model proteins denaturing after one freeze-thaw cycle [26]. Whereas comparable levels of denaturing were observed for samples frozen at a slower rate after 11 cycles, indicating surface triggered denaturing [26]. As for liposomes, the same adsorption phenomenon is observed leading to ruptured/leaky membranes after one freeze-thaw cycle [171]. Similar to the other stresses that occur during freezing, the addition of a stabilizer can quell these problems because instead of ice forming, a "glassy" structure forms when frozen mediating all the problems that ice formation causes.

In addition to the issues listed above when freezing biological samples, including MSC-EVs, their their long-term storage and transport can become a problem. For long-term storage, biological samples will have to be kept at -80ºC or -196ºC making it inconvenient and costly to keep a high quantity of MSC-EVs available. When transporting EVs the low temperature will have to be maintained by using dry ice/ice packs but if the package thaws during transport, it becomes useless. Therefore, several studies have been conducted to examine the viability of freeze-drying MSC-EVs to store them at room temperature.

2.12 Freeze-drying Extracellular Vesicles

Lyophilization is primary used in the pharmaceutical industry to store drugs and vaccines for an extended period of time while maintaining their biological activity [172]. Freeze-drying consists of four steps freezing, primary drying, secondary drying, and rehydration [172]. Primary drying removes all the frozen water while secondary drying removes the "bond" water that interacts with biomolecules [172]. Controlling all four steps is vital to ensure the dried product meets the defined Quality-by-Design (QbD) mandates. Lyophilization allows for biological samples to be stored at room temperature but creates multiple stresses that rupture lipid bilayer membranes and denature/degrade proteins at each step of the process.

2.12.1 Freezing Step

The strain biological samples experience while being frozen has already been detailed in section 2.11. Once the sample is frozen, it can enter the freeze dryer and start the drying steps to remove water from the sample.

2.12.2 Primary and Secondary Drying

During the primary drying phase, the sample is placed in a vacuum at a pressure ranging from 50 to 200 mTorr for sublimation of approximately 80% of the water [173], [174]. The duration of the primary drying phase depends on the structure of the ice crystals that form during freezing and the drying conditions [175]. The stability of the freeze-dried product relies on the temperature lyophilization is occurs. All biological samples have a glass transition temperature (T_g), and the T_g of a sample depends on the T_g of its different components; for pure water the T_g is -137^{o}C [176]–[178]. Samples that are lyophilized above their T_g will experience denaturing, aggregation, and vesicle fusion, therefore lyophilization should occur below the sample's T_g. (a more in depth look into T_g is in section 2.12.4.1) [177]. After primary drying the water that remains are the molecules that interact with the polar groups of the biomolecules known as bond water or residual

water. To remove these water molecules the sample will enter the secondary drying phase, where a similar vacuum is maintained but the temperature is increased, while kept below T_g, to facilitate water desorption [179], [180]. However, a certain amount of residual water, around 1%, must be retained as over drying can decrease protein, liposome, and EV stability [181]. If too much water remains after lyophilization aggregation, reconstitution issues, and loss of protein activity can occur [181]. The loss of protein function might be due to peptide bond hydrolysis that follows Figure 2, which will break down the peptide chain [182].

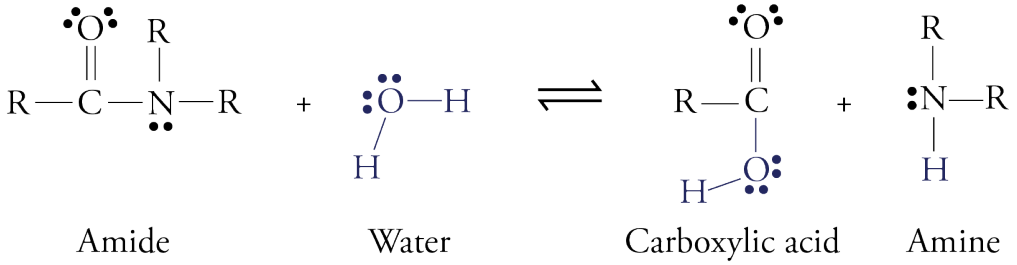

Figure 2. Hydrolysis of the peptide bond.

In terms of over drying, the removal of water molecules that interact with proteins and phospholipids bilayer can drastically affect their stability [183]. Protein stability and functionality is heavily influenced by the hydration shell that covers its surface [183]. The hydration shell's dynamic abilities play a vital role in peptide chain folding, enzyme activity, and protein recognition [183]. During secondary drying the hydration shell is removed which may cause the protein to denature [183]. Dried proteins are also inclined to transfer protons to the ionized carboxyl group causing the removal of any charge resulting in increased hydrophobic interactions leading to protein aggregation [183]. Furthermore, some enzymes require water molecules in their active sites, such as lysozymes, and after dehydration these enzymes loss their functionality [184]. The removal of residual water exposes protein to the environment and in particular molecular oxygen and light leading to decreased activity or protein content [185]. In the presence of light and oxygen peroxy radicals can form that will transform methionine to methionine sulfoxide and cysteines to

different sulfones and acids [185], [186]. While tryptophan groups that are excited by light can extract a hydrogen from nearby tyrosine groups and react with the peptide backbone leading to its cleavage. Furthermore, the excited tryptophan could also react with oxygen to form kynurenine or other hydroxylated derivatives [185], [187]–[189].

Over drying the membrane bilayer of liposomes or EVs will also cause drastic changes to the structure of the membrane. During the drying process water is removed from the headgroups of phospholipid bilayers packing them closer together, which in turn forces the alkyl chains closer to one another leading to increased Van der Waals interactions [190]. This causes the thin fluid layered membrane to transition to a "solid" state known as the gel phase, where the chains are rigid and fully stretched [191]. While in the gel phase the membrane can further transform into a hexagonal or cubic phase depending on the composition of the membrane, as seen in Figure 3 [192]. No matter which phase the membrane transitions to the same result occurs when rehydrated, a ruptured membrane.

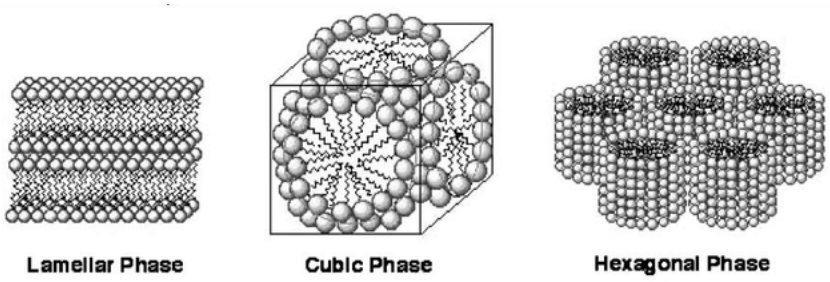

Figure 3. Different lyotropic mesophases of a phospholipid bilayer membrane. *Adapted from an image by Chemical Society Reviews* [193].

The removal of water also makes the oxidation of unsaturated phosphides possible. Oxidation is initiated by reactive oxygen and continues via the lipid peroxidation chain reaction seen in Figure 4, leading to a leaky or ruptured membrane [194].

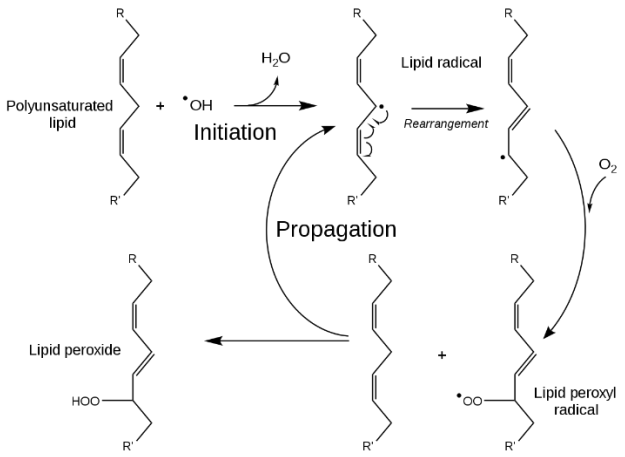

Figure 4. Lipid peroxidation chain reaction.

To decrease the stress caused during drying a cryoprotectant can be added that will replace water and interact with the polar groups of proteins and phospholipids. After secondary drying, the biological sample can be stored at room temperature for a long period of time and once needed the dried sample can be reconstituted with the appropriate solvent.

2.12.3 Rehydration

Reconstitution of the dried product is rarely discussed but is very significant for confirming stability and functionality of said product. The cake that forms could be visually great, but this does not indicate that the product is perfectly preserved once rehydrated. If the solvent used contains any components that were not in the original sample or if a different amount is used for reconstitution, osmotic shock could occur. Once rehydrated, the functionality of the product must be re-established to ensure clinical use is still viable and is stable long enough for administration [195]. To help stabilize biological samples throughout all steps of lyophilization the addition of a cryoprotectant will protect the sample.

2.12.4 Addition of Cryoprotectant can Stabilize Extracellular Vesicles and its content during Lyophilization

Sucrose, lactose and especially trehalose are very popular disaccharides that are used as cryoprotects or dehydration stabilizers for freeze drying. Their abilities were first identified in

several plants and animals that can survive while extremely dehydrated, where the common factor amongst these organisms is the high levels of disaccharides, in particular sucrose and trehalose [196]–[200]. As a result, multiple studies have been performed to identify any practical application leading to their use as an excipient in the pharmaceutical industry, a key ingredient for dried and processed foods, and used in vaccines and organ transplants as a non-toxic cryoprotectant [28].

It was initially believed that the sole mechanism disaccharides utilize for preservation of proteins and membranes is the formation of "glass", due to it lowering protein mobility and degradation [201], [202]. However, Crowe et al. had shown that freeze-drying liposomes in the presence of dextran and hydroxyethyl starch, good glass formers, did not preserve the liposomes once rehydrated [203]. The researchers suggested that in addition to forming glass, the incorporated disaccharide must form interactions with polar groups located on the protein or membrane. Therefore, to protect biological samples the cryoprotectant added should cause glass formation at higher temperatures during freezing and interact with the sample as water is removed during drying.

2.12.4.1 Glass Transition Temperature

The glass transition temperature (T_g) is a temperature range in which freezing an aqueous solution will ingrain biological components in a noncrystalline solid matrix delaying reactions involving degradation [204]. In terms of food preservation there is an established correlation with T_g, where food stored below T_g are more stable and above this temperature result in permanent changes [204]. Below T_g the molecular interactions, cooperativity, and mobility of biological samples are heavily restricted as the material is in paralyzed state [204]. The analogy is that the biological sample is embedded in glass. A biological sample's T_g is heavily influenced by its free water

content, where increasing free water decreases the sample's T_g and can be defined by the Gordon-Taylor equation for binary solutions [205, p. 3].

$$T_g = \frac{w_1 T_{g1} + k w_2 T_{g2}}{w_1 + k w_2} \quad (2)$$

Where w_1 and w_2 are the mass fraction of water and sugar respectively, T_{g1} and T_{g2} are the glass transition temperatures of pure water and sugar respectively, and k is the Gordon-Taylor constant which changes depending on the system.

Trehalose in particular is the best sugar for preservation of biological systems due to its high T_g, ranging from 79°C to 120°C [206]. As mentioned beforehand, water has a T_g of -137°C meaning a crystalline structure will only form below this temperature. By adding trehalose, the T_g of the mixture will increase greatly depending on the amount of trehalose added and the other components in the system [206]. Furthermore, trehalose also has the ability to form a dihydrate. Crowe et al. had shown that freezing liposomes in the presence of trehalose is better than sucrose because water molecules in the sample also become chemically bond to the dehydrate, thus preventing T_g from lowering [207]. Since sucrose does not contain a dihydrate water was allowed to remain free resulting in a lower T_g [207].

If choosing a cryoprotectant were only based on having a high T_g then dextran would be the better choose over trehalose. Dextran is a polymer of glucose that has a T_g ranging from 120°C to 180°C depending on its molecular weight [208]. However, trehalose was shown to be more effective because of the molecular interactions it forms with the biological system suggesting that T_g is not the only factor involved in preservation.

2.12.4.2 Molecular Interactions between Disaccharides and Biomolecules

It is believed that during the drying phase of lyophilization, disaccharides will form hydrogen bonds with the polar groups as water is removed resulting in preserving the structural integrity of

the biological sample [209]. The hydration shell surrounding proteins can be replaced by forming hydrogen bonds with disaccharides preventing any denaturing [209]. Any degradation reactions, i.e. hydrolysis or oxidation, are reduced as the groups involved are interacting with the disaccharide instead [209]. As for membranes, replacing water at the membrane-fluid interface will prevent the membrane from transitioning from the lamellar phase to the gel phase [209]. This theory was first introduced by Crowe et al. as water replacement theory and a depiction of how trehalose interacts with the membrane is seen in Figure 5 [209].

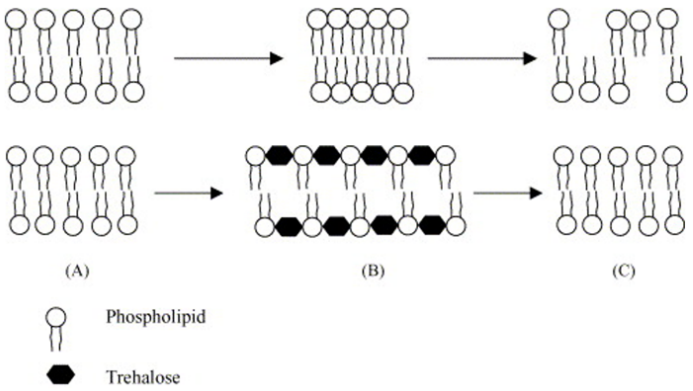

Figure 5. Depiction on how a phospholipid membrane is affected during freeze-drying. (A) the hydrated plasma membrane, (B) dehydrated membrane with or without trehalose, and (C) rehydrated membrane. Reprinted from Colloids and Surfaces B: Biointerfaces , Vol: 40, Alex Patist, Hans Zeorb, Preservation of Trehalose in food and biosystems, pg. 7, 2005, with permission from Elsevier [210].

Other disaccharides, such as maltose and sucrose, can also form hydrogen bonds but only provides partial stabilization when compared to trehalose and would require more to have an equivalent effect [211]. The interesting fact is that maltose, sucrose, and trehalose are chemical isomers, same chemical formula ($C_{12}H_{22}O_{11}$), but trehalose is the better cryoprotectant [212]. This is due to its chemical structure; trehalose is a more flexible molecule when compared to its monomer counterparts allowing it to conform around irregular shaped biomolecules to provide better interaction with its polar groups [211].

The combination of increasing the glass transition temperature of the solution and incorporating itself into the biological sample give trehalose its attractive cryoprotectant capabilities.

2.12.4.3 Trehalose as a Cryoprotectant for Extracellular Vesicles

Trehalose is a nonreducing and non-diffusing sugar made from two glucose molecules that are bonded together by a 1,1-glycosidic linkage [213]. This naturally occurring sugar is found in plants, spores, fungi, vegetative cells, bacteria cells, and insects [213]. The presence of trehalose allows these organisms to survive in extreme cold or complete dehydration, which prompted their use as a cryoprotectant for proteins and cells [213], [214], [215].

One of the first instances of lyophilizing MSC-EVs with trehalose was performed by Frank et al. They first loaded the MSC-EVs with glucuronidase and freeze-dried them with 0.5% to 4% (w/v) trehalose [27]. It was observed that after lyophilization that some level of aggregation still occurred and that glucuronidase activity increased as the amount of trehalose in the freeze-dried sample increased [27]. While Charoenviriyakul et al. had lyophilized B16BL6 derived EVs with 50 mM of trehalose while frozen with liquid nitrogen and noticed the absence of trehalose resulted in EV aggregation, while the addition of trehalose negated the aggregation [216]. They also loaded their EVs with glucuronidase and found that its activity was retained post lyophilization; they even administered their loaded rehydrated EVs into mice and found little change in its pharmacokinetics when compared to administering fresh EVs [216]. Baradie et al. had reported that lyophilized EVs isolated from adipose-derived stem cells inhibited hypoxia-induced muscle cell injury [29]. This group had lyophilized their EVs with a combination of trehalose and polyvinylpyrrolidone 40 (PVP 40) and found that without these cryoprotectants there was a significant drop in particle count [29]. To assess if bioactivity is retained, they treated hypoxia cultured human myoblasts with 50

μg/mL of rehydrated EVs and observed that EVs freeze dried in the presence of their cryoprotectant formula were able to reverse the muscle cell injury induced by hypoxia [29].

Trehalose has been shown to be a very capable cryoprotectant in preserving the structure and therapeutic functionality of biomolecules. However, trehalose has also been shown to have its own therapeutic abilities for treatment with neurodegenerative diseases.

2.12.4.4 Neuroprotective Capabilities of Trehalose

In addition to cryopreservation studies, trehalose has been used in animal studies for neurodegenerative diseases, such as Parkinson (PD) and Huntington diseases (HD) [217]. The mechanism utilized by trehalose is theorized to be the activation of autophagy *in vivo* [217]. Autophagy is a biological pathway that removes damaged cellular elements via lysosomes [218]. This includes damaged organelles, misfolded and aggregated proteins. A study that orally administered trehalose to PD mouse model led to a decrease in autophagic substrate, p62/SQSTM1, resulting in the removal of toxic proteins and inhibition of cell death [219]. In another study involving PD mice they reported that trehalose prevented the reduction of dopamine in the striatum and inhibited gliosis, a process that leads to scaring in the CNS as a response to CNS damage [220]. From a study orally treating HD mouse models with trehalose they observed an improvement in motor function and a prolonged lifespan when compared to control mice [221].

3 Materials and Methods

3.1 Sample Preparation

MSC-EVs were generously provided by Health Canada's stem cell – based therapeutics laboratory regulatory research division. Once received, the MSC-EV sample is separated into 5 aliquots and an equal volume of a stock trehalose dihydrate (VWR Cat#K480-25G) solution is added so that the trehalose concentration for the aliquots are either 0, 50, 100, or 200 mM and incubated for 1 hour at 4^{o}C for integration into the membrane. The aliquots are then frozen at -80^{o}C overnight and

lyophilized using the Labconco FreeZone 6plus (Cat# 7934024) for 48 hours. After two weeks of storage at room temperature the dried aliquots are rehydrated with an equal amount of distillated water that was filtered with a 50 nm hydrophilic membrane (Whatman Cat# 110603) and analyzed.

Once the optimum trehalose concentration was determined from the above experiments, the optimum freezing conditions was tested. The MSC-EV sample was aliquoted as before but this time equal volumes of the trehalose bulk solution was added to achieve the optimum trehalose concentration. This time the aliquots were frozen at one of the following conditions -1°C/min via Mr. Frosty (Nalgene Cat# 5100-0001), -20°C, -180°C, and -196°C (liquid nitrogen). There samples were then dried, stored at room temperature, rehydrated after two weeks, and analyzed the same as before.

3.2 Determining the Total MSC-EV Protein Concentration

Lysate preparation follows an already established protocol with slight modifications [222]. Briefly, 500 µL of the MSC-EV sample, fresh or rehydrated, was mixed with an equal volume of RIPA lysis buffer (Thermo Scientific Cat#89900), instead of resuspending an EV pellet, and set to incubate at 4°C for 30 minutes. The sample was then sonicated (Qsonica model# Q700) at an amplitude of 20% for 10 seconds 3 times with 30 second rest periods on ice in between pulses. The sample was then centrifuged at 2000 xg for 5 minutes. The protein content of MSC-EVs was then determined by using a micro–BCA Protein Assay Kit (Thermo Scientific Cat#23235) according to the manufacturer's instructions and using BSA as the standard.

3.3 NTA analysis of fresh and rehydrated MSC-EVs using NanoSight NS300

MSC-EVs were analyzed by NTA using the NanoSight NS300 (Malvern Panalytical). Following EV purification from EV-rich cell conditioned media (CCM), the EV pellet was resuspended in filtered D-PBS$^{-/-}$ (ThermoFisher Cat#10010-023) and sterilized via 0.2 um acrodisc syringe filter

(Sigma Aldrich Cat#PN4612). Then 150 microliters of the EV-rich sample was diluted by 10x in filtered D-PBS$^{-/-}$ to obtain a final volume of 1.5 mL. Each sample was vortexed prior to filling the syringe and a syringe pump was used for acquisition in flow mode. Each run used the following script: six captures of 1 minute at speed 10 under flow mode. The capture settings had a camera level and detection threshold of 12. In between each ample, 3 mL of filtered water and ethanol was used to wash the system. The raw data was analyzed using the NTA 3.0 software where analysis of 5 out of the 6 captures was performed to obtain the estimated total EV concentration, size, and distribution. The MSC-EV particle concentration and the concentration at every size distribution was multiplied by the appropriate dilution factor to obtain the accurate MSC-EV concentration. Once the dried MSC-EVs were rehydrated with filtered distilled water, the samples were analyzed using the same script, camera level, and detection threshold, but were not diluted.

3.4 Transmission Electron Microscopy (TEM) of MSC-EVs

Sample preparation for TEM analysis followed an already published protocol [222]. Briefly, 300 µL of fresh or rehydrated MSC-EVs suspension was filtered with vivaspin filters (VWR Cat# CA76409-010) after being rinsed with 200 µL of filtered PBS centrifuged at 2000xg for 3 minutes. The concentrated MSC-EVs was diluted with 4% paraformaldehyde (PFA, ThermoFisher Scientific Cat# J61899.AK) to a volume of 300 µL. Then, 50 µL of MSC-EV fixed with PFA was placed on parafilm and carbon coated electron microscopy grids (Electron Microscopy Sciences Cat# CF300-CU), which were glow discharged (Quorum, GloCube plus), were inverted onto the droplet and allow to incubate for 5 minutes. Grids were then blotted with filter paper and left to dry for 1 hour at room temperature before imaging. The imaging was done using a JEOL JEM-1400 series operating at 120 kV.

3.5 Tube Formation Assay

To observe whether the rehydrated MSC-EVs retain their angiogenic capabilities a tube formation assay was performed following a predetermined protocol with slight modifications [223]. Human umbilical vein endothelial cells (HUVECs) were first cultured in T-75 flasks (Sigma Aldrich Cat# 83.3911) with F-12K media (ATCC 30-2004) supplemented with 10% FBS (ATCC Cat# 30-2020), 30 µg/mL of Corning™ Endothelial Cell Growth Supplement (Fisher Scientific Cat# CB-40006), and 0.1 mg/mL of Heparin (Sigma Aldrich Cat#H3393). Once the confluence of the flasks reaches 70% to 80% the HUVECs were passaged with trypsin – EDTA (ThermoFisher Cat#25300062). HUVECs of passages ranging from 3 to 5 (ATCC Cat# CRL-1730) were seeded at a density of 15,000 cells/well in a 96-well plate (Costar Cat#3628) that were coated with 50 µL of growth-factor reduced, without phenol red ECM Gel (Sigma-Aldrich Cat# E6909-5ML). HUVECS were treated with rehydrated MSC-EVs that were lyophilized in the presence of 100 mM of trehalose at a total protein concentration of either 50, 100 or 200 µg/mL as these concentrations have shown to promote tube formation [118], with 100 µg/mL of rehydrated MSC-EVs that were lyophilized without trehalose, with F-12K medium (ATCC 30-2004) as control, and with 100 mM of trehalose in PBS as a negative control. Cells were incubated at 37°C and 5% CO_2 for 10 hours. Images were taken using Axio Observer Z1 (Zeiss) and processed using the Zen 3.2 software. The tube characteristics were analyzed using ImageJ to determine the number of branches and their length.

3.6 Primary Neural Stem/Progenitor Cell (NSPC) co-culture with rehydrated MSC-EVs

To analyze whether the rehydrated MSC-EVs retain their therapeutic abilities, they were used to treat primary NSPCs to stimulate proliferation as previously described [18]. 6- to 12-week-old adult mice (Strain B6/129S) were sacrificed using CO2 and cervical dislocation and NSPCs were

harvested from the SVZ of the mice brain. The cells were then seeded into a 6-well plate at a concentration of 20,000 cells/mL and incubated at 37°C, 5% CO_2, 21% O_2. The NSPCs were cultured in serum free media (SFM) consisting of low glucose DMEM/F-12 at a 1 to 1 ratio (ThermoFisher, Cat# 11320033), 30% glucose (ThermoFisher, Cat# 15023021), 7.5% $NaHCO_3$ (ThermoFisher, Cat#25080094), 1 M HEPES (ThermoFisher, Cat# 15630080) and supplemented with 2mM L-glutamine (Lonza, Cat# 17-605E), 100 µg/mL penicillin-streptomycin (Lonza, Cat# 17-602E), 2 µg/mL Heparin and 1X B27 (ThermoFisher Scientific Cat# 0080085SA). NSPCs in SFM were then treated with rehydrated MSC-EVs that were lyophilized in the presence of 100 mM of trehalose at a total protein concentration of either 50, 100 or 200 µg/mL, with 100 µg/mL of rehydrated MSC-EVs that were lyophilized without trehalose, with 100 mM of trehalose in PBS as a negative control, and with 20 ng/mL of FGF2 (peprotech Cat# 100-18B) and EGF (VWR Cat# CACB354052) as a positive control. Neurospheres were then imaged using Zeiss Axiovert 200M inverted microscope and their diameter and quantity were analyzed using ImageJ.

To test the multipotency of neurospheres treated with rehydrated MSC-EVs, NSPCs were transferred to 4-well Lab-Tek Chamber slides (ThermoFisher Scientific Cat# 177399PK) coated with laminin (Fisher scientific Cat#354232) and poly-L-ornithine (Sigma-Aldrich Cat# P4957). They were left to differentiate for 7 days by adding 1% FBS in SFM. Finally, the cells were fixed with 4% PFA after 7 days of culture and were immune stained as decided below.

3.7 Immunostaining of differentiated NSPCs

To identify cell differentiation, the processed NSPCs as decided above were stained for makers associated with differentiated progeny. Briefly, differentiated cells were blocked and permeabilized with 10% normal goat serum (NGS, Fisher Scientific Cat# 10000C) and 0.3% triton X-100 (Fisher Scientific Cat# BP151-100), respectively, for 1 hour at room temperature, and subsequently incubated with primary antibody in 10% NGS at 4°C overnight. The following

primary antibodies were used: βIII-tubulin (1:500) (ThermoFisher Cat# PA5-85639) for neurons and glial fibrillary acidic protein (GFAP) (1 mg/mL) (ThermoFisher Cat# PA1-10004) for astrocytes. After washing with PBS three times, the samples were incubated with the secondary antibodies Alexa 488 (ThermoFisher Cat#A48282) and Alexa 555 (ThermoFisher Cat#A-21437) for βIII-tubulin and GFAP, respectively, in 2% NGS for 1 hour at room temperature and washed with PBS three times. As for oligodendrocytes, O4 (15 mg/mL) (Millipore Sigma Cat# O7139-50UG) primary antibody was used but this marker is on the membrane, therefore these cells were not permeabilized with 0.3% triton-X. These samples were then incubated in Alexa 647 (ThermoFisher Cat#A-21238) in 2% NGS for 1 hour at room temperature and washed with PBS 3 times. All samples were counterstained with Hoechst (1:2000) (ThermoFisher Cat# H3570) for 5 minutes at room temperature [18]. The cells where then imaged using Zesis Axio Observer 7 and images were processed using the Zen 3.2 software and ImageJ.

3.8 Statical Analysis

All statistical analysis was carried out via Prism 9 using a one-way ANOVA followed by Tukey multiple comparison test. P-values < 0.05 were considered statistically significant.

4 Results and Discussion

To narrow down the optimum freeze-drying conditions, this work tested multiple trehalose conditions and freezing temperatures. First, MSC-EV samples had trehalose concentrations of 0, 50, 100, or 200 mM and then frozen at -80°C before lyophilization. Then to determine the optimum freezing temperature, MSC-EVs were frozen at -1°C/min, -20°C, -80°C, and -196°C (liquid nitrogen) in the presence of the optimum trehalose concentration. Once the ideal conditions were determined the biological activity of the rehydrated MSC-EVs was tested by performing a tube formation assay and co-culturing them with NSPCs. A flow chart, seen in Figure 6, outlines the experimental procedure.

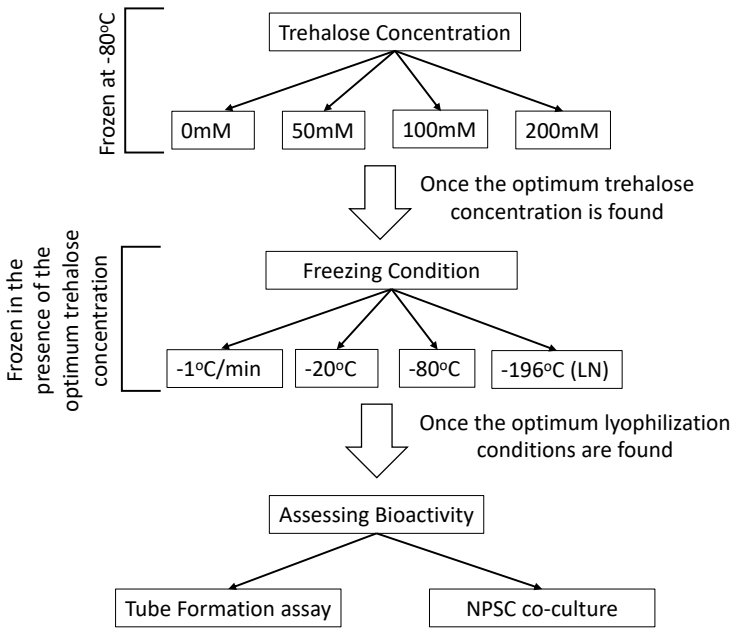

Figure 6. Flow chart depicting the experimental design throughout the project.

4.1 Determining the optimum trehalose condition

4.1.1 Size distribution of fresh and rehydrated MSC-EV by nanotracking analysis (NTA) using NanoSight NS300

As suggested by the minimal information for studies of extracellular vesicles (MISEV) NTA quantification is essential for characterizing EVs [103]. Once the MSC-EVs were produced, an aliquot was quantified by NTA using Nanosight (NS300), at a camera level of 12 and a detection threshold of 12, to determine the size distribution, mean size, mode size, and particle concentration. The rest of the sample was then separated into 5 aliquots and equal volumes of a double filtered (DF) trehalose solution was added to achieve trehalose concentrations of 0, 50,100, and 200 mM. These samples were then frozen at -80°C overnight and lyophilized for 48 hours using the Labconco FreeZone 6 plus freeze dryer. The aliquots were then stored at room temperature for 2 weeks and rehydrated with DF distillated water to the volume they were frozen at. NTA was then repeated, at the same parameters, and compared to the results from the fresh aliquot, as seen in Figure 7.

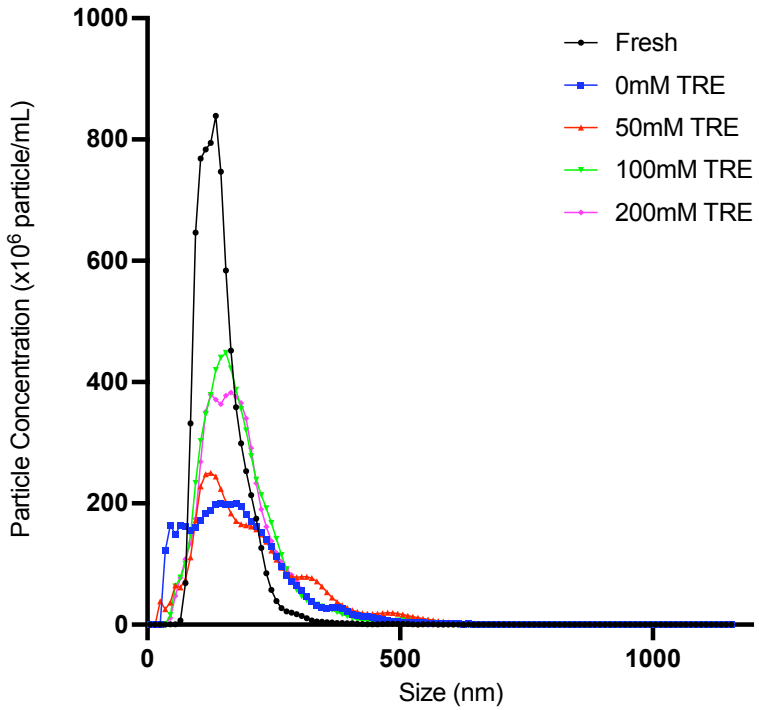

Figure 7. MSC-EVs were characterized by NTA as a method to determine particle concentration and size distribution of fresh MSC-EVs and rehydrated MSC-EVs containing increasing amounts of trehalose. X-axis denotes the size (nm) and the y-axis denotes the particle concentration (particles/mL). This experiment was performed with 1 healthy donor with 4 independent trials.

From the NTA the fresh samples had an average size ranging from 100 nm to 250nm, which is consistent with MSC-EV sizes reported in literature [103]. As for the freeze-dried samples, no matter the amount of trehalose added there is still some level of aggregation occurring post lyophilization, which is indicated by a wider size distribution, for the 0 and 50 mM samples, and a slight shift of the distribution to the right, for the 100 and 200mM samples. The sample with no trehalose was frozen at -80°C but has a glass transition temperature ranging from -139°C to -135°C [204]. Since the freezing temperature is greater than the T_g of the solution, the MSC-EVs in the sample have more mobility and are not in a "glassy" state allowing the EVs to aggregate resulting in a wide size distribution. Additionally, the absence of trehalose allows the MSC-EV membrane to transition to the gel, cubic, or hexagonal phase and once rehydrated the membrane will breakdown, as suggested by Kumar *et al*. [192]. As for the 50 mM sample, the size distribution of

the MSC-EVs start to become more narrow but not enough trehalose has been added as multiple peaks can still be observed suggesting that the T_g of the solution could still be lower than -80^{o}C and more trehalose should be added. The size distribution for the samples with 100 mM and 200 mM of trehalose are the closest to the fresh sample indicating that the amount of trehalose added was enough to minimize aggregation. Furthermore, both size distributions are very similar, with one predominate peak and one smaller peak. Both samples have similar size distributions indicating that increasing the trehalose concentration past 100 mM does not provide any further benefits. Another noticeable change is the shifting of the peaks to the right signifying that the majority of MSC-EVs have increased in size. The increase in size is further justified by the increase in mean and mode MSC-EV diameter seen in Figure 8.

4.1.2 Size Range of fresh and rehydrated MSC-EVs by NTA

In addition to size distribution, NTA can determine the mean and mode size of the analyzed samples. The fresh samples had a mean particle diameter of (mean ± SD) 172.35 ± 5.87 nm and a mode size of (mean ± SD) 126.58 ± 20.36 nm. However, post lyophilization there is an increase in MCS-EV diameter no matter how much trehalose is added. According to the MISEV guidelines the fresh samples are categorized as small EVs (100 to 200 nm), while all the rehydrated samples have a diameter greater than 200 nm classifying them as medium/large EVs. For samples with low trehalose concentration, 0 mM and 50 mM, the increase in size could be due to aggregation or vesicle fusion that occurs while the samples are stored at a temperature that is above T_g resulting in the MSC-EVs being mobile when in a frozen state [204]. Another reason for the increase in size, especially for the 100mM and 200mM samples, can be contributed to trehalose integrating into the membrane of the MSC-EVs, as seen in Figure 5, resulting in the extension of the membrane length. The only significant difference observed was the mode size between the fresh

and 100mM sample (*p*-value: 0.01). To further investigate how freeze-drying affects MSC-EVs, particle concentration was examined as seen in Figure 9.

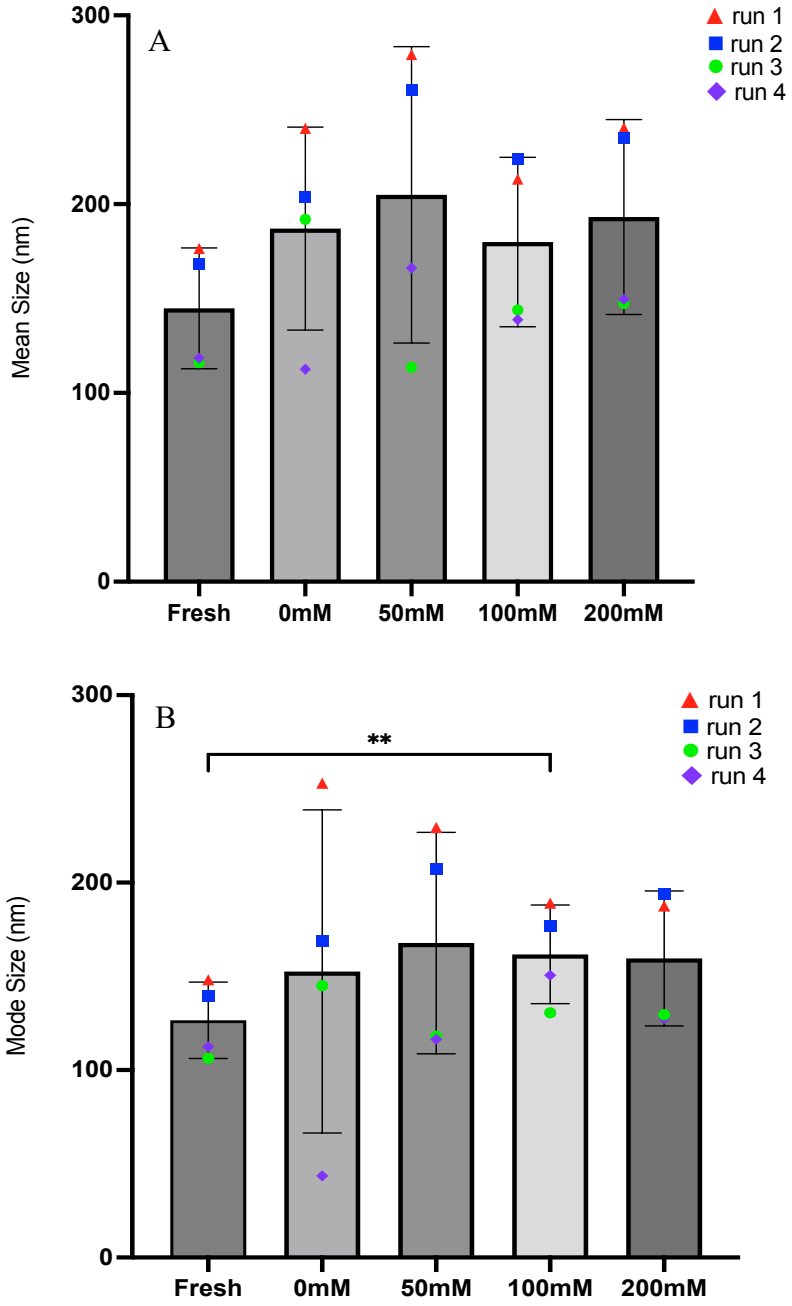

Figure 8. MSC-EVs were characterized by NTA to determine the mean EV diameter. The X-axis denotes the trehalose concentration (mM) of the sample and the Y-axis is the measured diameter (nm). (A) is the average mean diameter, and (B) is the average mode size. A one-way ANOVA followed by a Tukey multiple comparison test was used for statistical analysis. Data presented as mean ± SD, n = 4. ***p*<0.01.

4.1.3 The effect of lyophilization on MSC-EV particle concentration

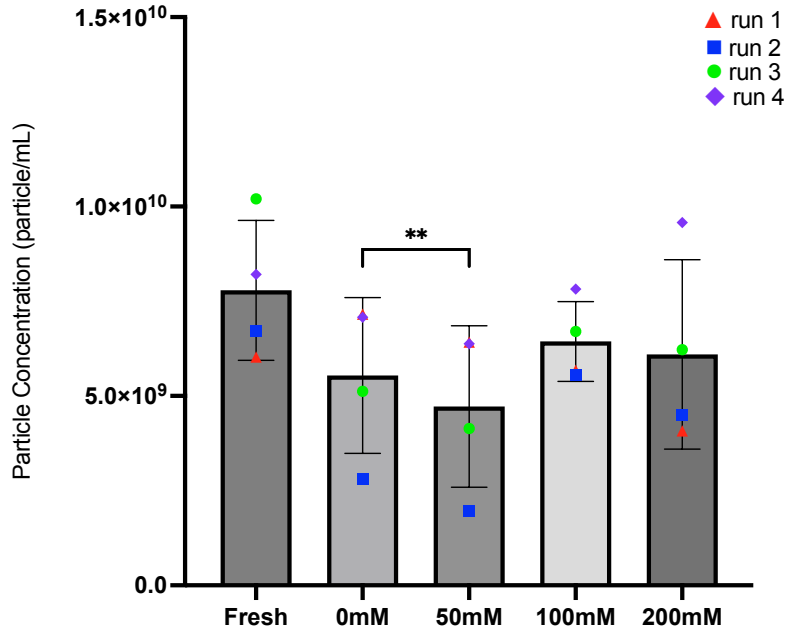

Figure 9. Mean particle concentration of MSC-EVs by NTA. The X-axis denotes the trehalose concentration (mM) of the sample and the Y-axis is the mean particle concentration (particle/mL). A one-way ANOVA followed by a Tukey multiple comparison test was used for statistical analysis. Data presented as mean ± SD, n = 4, $^{**}p<0.01$

From NTA analysis the fresh samples had a particle concentration of (mean ± SD) $6.38\text{x}10^{9}$ ± $4.88\text{x}10^{8}$ particle/mL while all the rehydrated samples experienced a decrease in particle concentration. The decrease in particle concentration during the freeze-drying process, as mentioned above, can be due to aggregation because of the lack of trehalose in the 0 mM and 50 mM samples, as the Nanosight NS300 would recognize a cluster of particles as one large particle, which can also contribute to the larger particle diameter. The EV aggregation could have also occurred during the freezing step when liquid-liquid phase separation happens leading to a higher MSC-EV count in one of the phases causing aggregation [169]. In addition to aggregation, the decrease in particle concentration could have been caused by the rupturing of MSC-EVs due to osmotic shock as the solute concentration changed during freezing. A drastic change in pH could have also occurred, which has shown to decrease particle concentration [162]. The samples with

low amount of trehalose could have also formed ice crystals that would have physically ruptured the EVs by creating an ice-water interface during freezing causing cells to diffuse and breakdown at this interface [171]. Another reason for the loss of particles could be explained by the lack of integration between trehalose molecules and the membrane. As seen in Figure 5, in the absence of trehalose the membrane will start to breakdown during the drying phase as the residual water is removed leading to the complete breakdown of MSC-EVs resulting in lower particle concentrations [192]. While the samples with 0 and 50 mM of trehalose were lyophilized and stored at room temperature, the lack of protection from trehalose could have caused the lipids in the MSC-EV membrane to oxidize according to the reaction mechanism seen in Figure 4 [194]. Finally, during the rehydration process the MSC-EVs could have experienced osmotic shock resulting in either the MSC-EVs bursting or shrivel up [195]. The only significant difference observed was between the 0mM and 50mM sample (p-value: 0.0039).

After characterization of MSC-EVs with Nanosight, the total protein concentration was determined via microBCA assay, as the total protein amount contributes greatly to the therapeutic capabilities of MSC-EVs.

4.1.4 Total Protein Concentration of Rehydrated MSC-EVs

The next step in characterizing MSC-EVs is determining the total protein concentration via microBCA assay. A fresh aliquot of MSC-EVs was mixed with an equal volume of RIPA buffer for EV lysis. Sonication was then performed with a Qsonica Q700 sonicator with a microtip equipped at an amplitude of 30 for 10 seconds and rested for 30 seconds. This was repeated 3 times and all samples were kept on ice throughout the sonication. The same process was then repeated for all rehydrated MSC-EV samples. Figure 10 shows how different levels of trehalose can influence protein concentration of MSC-EVs that have been lyophilized.

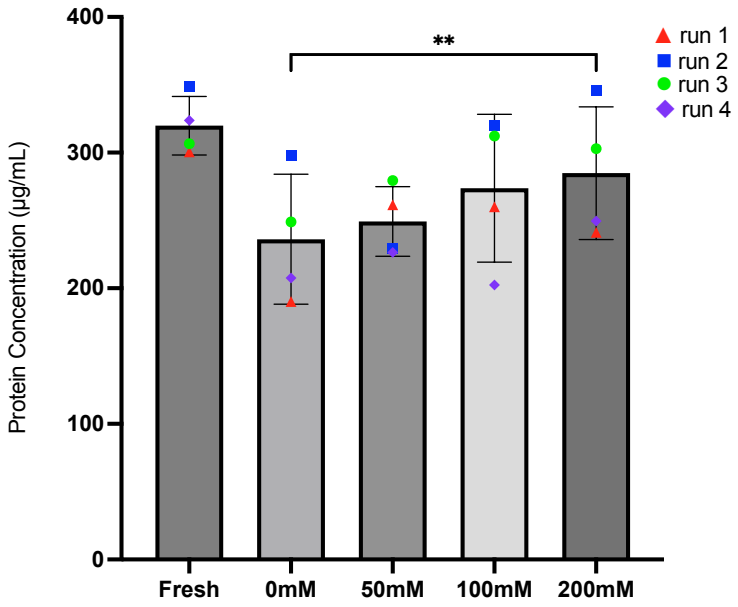

Figure 10. The total protein concentration (µg/mL) of MSC-EVs determined by a microBCA assay. A one-way ANOVA followed by a Tukey multiple comparison test was used for statistical analysis. Data presented as mean ± SD, n = 4. ** $p<0.01$.

The average protein concentration of the fresh MSC-EVs was found to be 324.59 ±34.03 µg/mL while the average protein concentration for all rehydrated samples were lower. The only significant difference observed was between the 0mM and 200mM samples (p-value: 0.0014). To explain why the protein concentration was lowered, the mechanism on how the microBCA assay detects protein needs to be understood. The microBCA assay depends on two reactions. First, four peptide bonds reduce Cu^{2+} ions, at a temperature of 37°C, to Cu^{+} in a Biuret reaction, as seen in Figure 11. The amount of Cu^{+} produced is directly related to the amount of protein present in the sample.

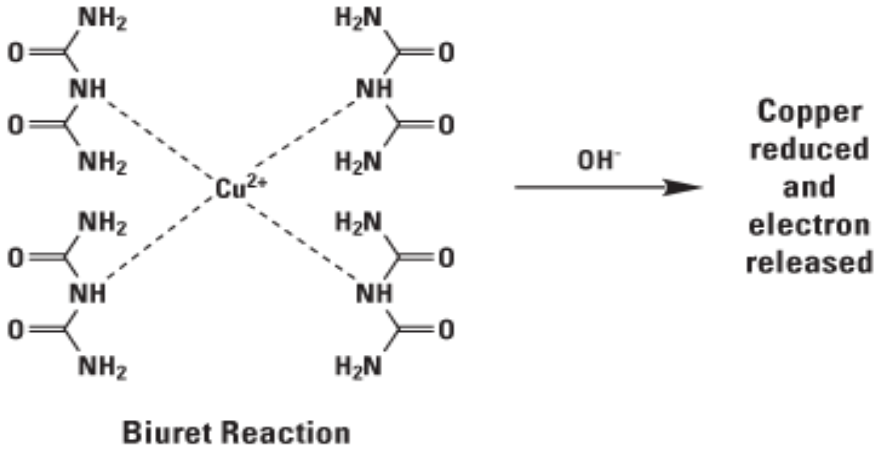

Figure 11. The Biuret reaction that reduces Cu^{2+} to Cu^{+} when interacting with peptide bonds.

A chelate is then formed between the Cu^{+} and two molecules of bicinchoninic acid (BCA), which forms a purple product that absorbs light at a wavelength of 562 nm, as seen in Figure 12.

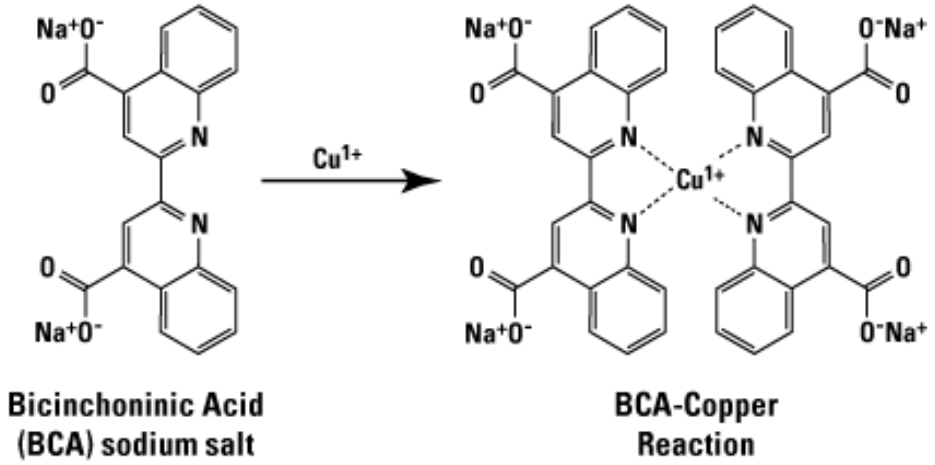

Figure 12. Chelate that forms between BCA molecules and Cu^{+}.

The BCA assay requires an intact peptide bond to quantify the protein content and will not detect small peptide chains or amino acids. Therefore, the MSC-EV samples with a 0 and 50 mM of trehalose could have their peptide chains broken down due to the lack of protection by trehalose leading to hydrolysis by residual water, seen in Figure 2. Another instance where peptide bonds can be broken down is while the MSC-EVs are stored at room temperature. The tryptophan groups

found along the peptide chain can be excited by light which can extract a hydrogen from a nearby tyrosine resulting in the cleavage of the neighbouring peptide bond [185]–[189]. Without trehalose protecting peptide bonds from these reactions' amino acids and small peptide chains will form that will not participate in the micoBCA assay leading to a lower protein concentration.

To observe if trehalose protects the structural integrity of MSC-EVs transmission electron microscopy (TEM) was performed.

4.1.5 Structural Integrity of Fresh and Rehydrated MSC-EVs

An aliquot of fresh or rehydrated MSC-EVs was concentrated using a vivaspin tube to remove solvents and other small molecules. The MSC-EVs were then fixed with 4% paraformaldehyde (PFA) and set on 300 mesh carbon film grids. The grids were then imaged with JEOL JEM-1400 series operating at 120 kV, as seen in Figure 13.

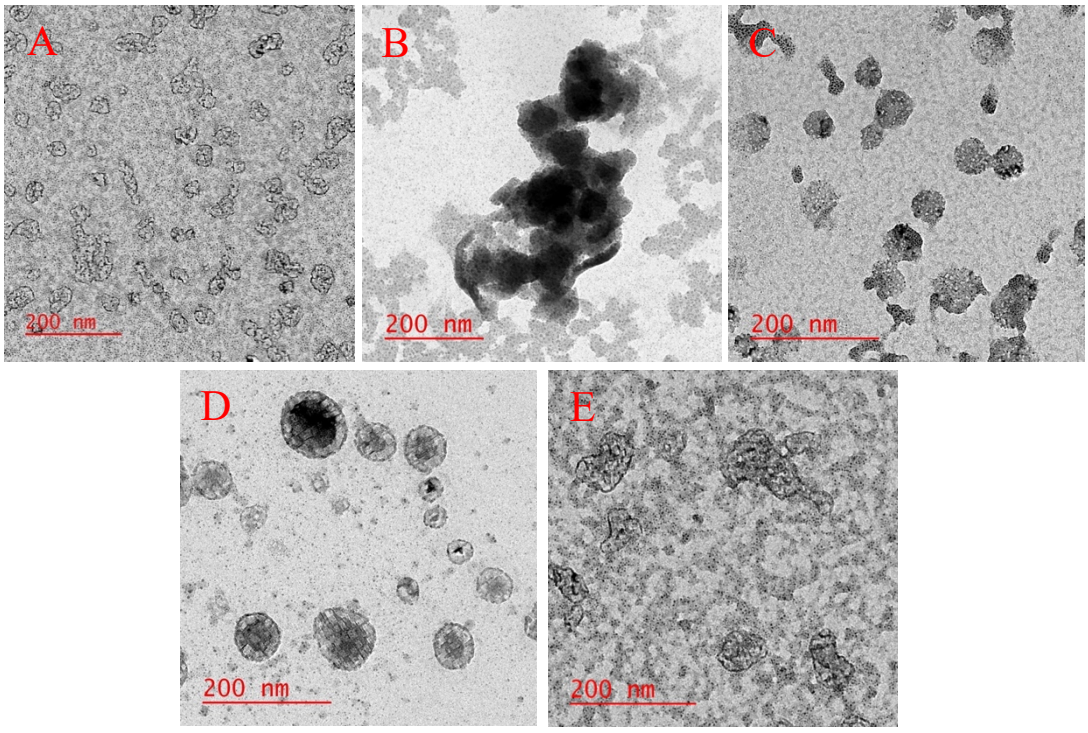

Figure 13. TEM images of (A) Fresh MSC-EVs, or rehydrated MSC-EVs that were lyophilized in the presence of (B) 0 mM, (C) 50 mM, (D) 100 mM, or (E) 200 mM of trehalose.

TEM was used to visualize the morphology of the MSC-EVs and help identify if the EV bilayer membrane is still intact. The idealized morphology of MSC-EVs was observed for the fresh EVs and EVs lyophilized with 100 and 200 mM trehalose. However, the TEM image for MSC-EVs lyophilized without trehalose (0 mM) is a cluster of EVs further providing evidence that a lack of trehalose results in aggregation of EVs. As for the MSC-EV sample freeze-dried with 50 mM of trehalose no bilayer membrane could be observed, which could be due to the membrane breaking down during the freeze-drying process. As for the 100 and 200 mM samples the MSC-EVs are still spherical in shape, their lipid bilayer is still intact, and their size corresponds to small EVs, suggesting that the trehalose is protecting the MSC-EVs during lyophilization.

These results show that when enough trehalose is added to MSC-EVs that will be lyophilized, trehalose will minimize their aggregation, protect their protein content, and maintain their structural integrity once rehydrated, which is consistent with what was been reported in literature [27], [29], [216]. As for determining the optimum trehalose concentration, it is evident that a concentration of 100 mM is when the full protective capabilities of trehalose can be observed. Therefore, a trehalose concentration of 100 mM would be the optimum choice and a larger concentration would result in diminishing returns. Therefore, the chosen trehalose concentration was 100 mM and was used for future experiments.

4.2 Determining the Optimum Freezing Conditions

4.2.1 Size distribution of fresh and rehydrated MSC-EV frozen at different temperatures by nanotracking analysis (NTA) using NanoSight NS300

Now that the ideal trehalose concentration was decided, this study then observed how different freezing temperatures could affect the stability of lyophilized MSC-EVs. EVs were frozen at a temperature of -1°C/min, -20°C, -80°C, or -196°C in the presence of 100mM and freeze dried for 48 hours. After two weeks of storage at room temperature, the powdered MSC-EVs were

rehydrated with double filtered distilled water and the same analysis was performed as seen in section 4.1 and the results are shown below in Figure 14.

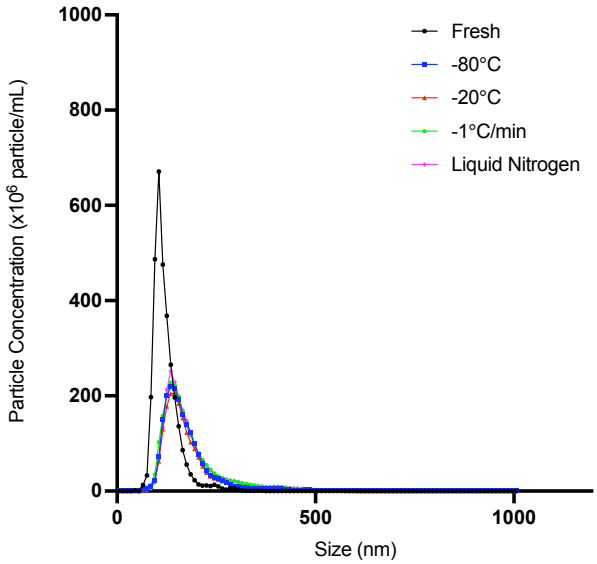

Figure 14. MSC-EVs were characterized by NTA as a method to determine particle concentration and size distribution of fresh MSC-EVs and rehydrated MSC-EVs containing increasing amounts of trehalose. X-axis denotes the size (nm) and the y-axis denotes the particle co concentration (particles/mL). This experiment was performed with 1 healthy donor with 4 independent trials.

The size distribution of the fresh sample has a range of 100 to 200 nm, which is similar to the fresh size distribution seen in Figure 7 and what has been reported in literature [103]. As for the lyophilized samples, the size distributions are similar amongst all freezing conditions and the 100 and 200 mM distributions seen in Figure 7, with a size range of 100 to 250 nm. The attributed shift in distribution could be similar to what happened before hand where trehalose would increase the size of the EVs once it incorporates itself into their membrane [209]. These results also suggest that different freezing conditions do not affect the size distribution of rehydrated MSC-EVs lyophilized in the presence of 100 mM. When freezing an aqueous solution, the temperature rate has a significant effect on the ice crystal formation, slower freezing rates result in smaller crystals forming and the opposite is observed at higher rates [147]. However, the addition of 100 mM of

trehalose forms a glassy like structure when frozen negating the formation of ice crystals and its negative effects on MSC-EVs.

As a result, it was initially believed that samples frozen at a higher temperature (ie. -1°C/min) would give more time for trehalose to incorporate into the membrane when compared to samples frozen at a lower temperature (ie. -196°C). Since this is not occurring, the 1-hour incubation time allows trehalose to integrate into the membrane resulting in maximum possible protective capabilities. To utilize the full protective potential of trehalose, literature suggest that the molecule should be present on both side of the membrane. Since trehalose cannot diffuse through the membrane of cells, there has been multiple methods developed to get trehalose into the intracellular space, such as microinjection, thermal shock, or ultrasound [214].

4.2.2 Average Diameter of Fresh and lyophilized MSC-EVs Frozen at Different Temperatures Quantified by NTA

Similar to the results presented in Figure 8, an increase in mean and mode particle diameter is observed, as seen in Figure 15.

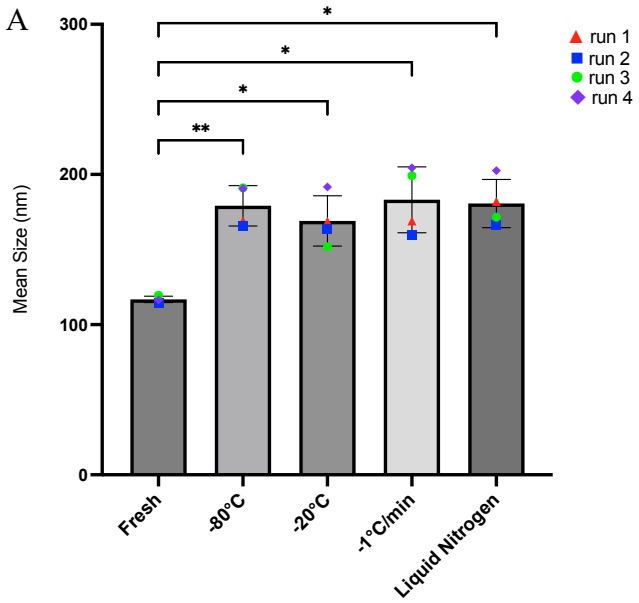

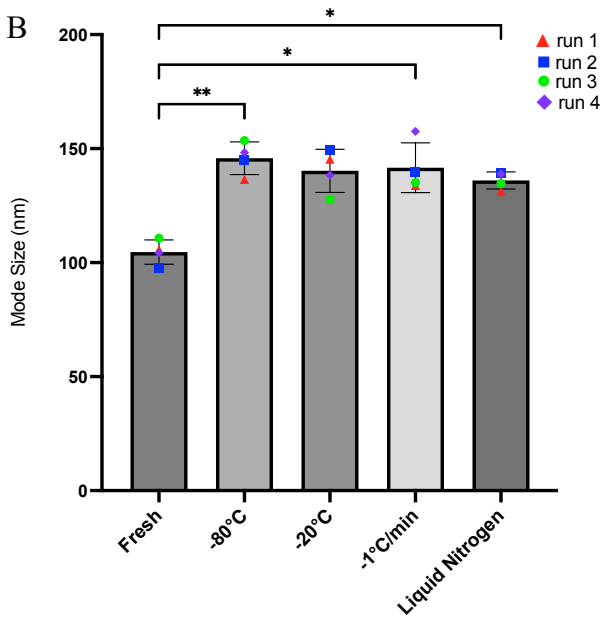

Figure 15. MSC-EVs were characterized by NTA to determine the mean EV diameter. The X-axis denotes the freezing temperature of the sample and the Y-axis is the measured diameter (nm). (A) is the average mean diameter, and (B) is the average mode size. A one-way ANOVA followed by a Tukey multiple comparison test was used for statistical analysis. Data presented as mean ± SD, n = 4, *p<0.05, **p<0.01.

NTA had determined that the mean and mode particle diameter for fresh MSC-EVs was 116.85 ± 2.14 nm and 104.65 ± 5.32 nm, respectfully, which is consistent with small EVs as reported by the MISEV [103]. When comparing sizes of fresh MSC-EVs from Figure 8, the mean and mode diameter is larger which could be due to donor-to-donor variability [74]. As for the rehydrated MSC-EVs, the particle diameter increases significantly (all p-values less than 0.05) to values greater than fresh MSC-EVs no matter the freezing condition. The significant increase in diameter could be due to the integration of trehalose into the MSC-EV membrane increases the particle diameter or some level of aggregation still occurs during the freezing or rehydration phase [209]. Moreover, no significant difference was observed when comparing the diameters of MSC-EVs between the different freezing conditions. This further provides more evidence that no individual freezing temperature has an advantage or disadvantage on the stability of rehydrated MSC-EVs

when freeze-dried in the presence of 100 mM of trehalose. The final analysis performed by NTA was the mean particle concentration as seen in Figure 16.

4.2.3 Average Particle Concentration of Fresh and lyophilized MSC-EVs Frozen at Different Temperatures Quantified by NTA

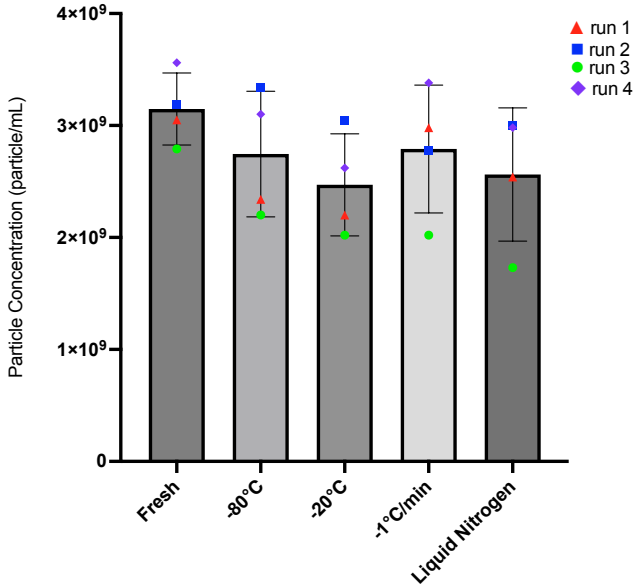

Figure 16. Mean particle concentration determined by NTA. The X-axis denotes the freezing temperature of the sample, and the Y-axis is particle concentration (particle/mL). A one-way ANOVA followed by a Tukey multiple comparison test was used for statistical analysis. Data presented as mean ± SD, n = 4.

NTA determined that the mean particle concentration for the fresh sample was $3.15x10^9 \pm 3.21 x10^8$ particle/mL. While all rehydrated samples had a mean particle concentration lower than the fresh sample, no significant difference was observed, p-values greater than 0.05. Since no significant difference was seen between the fresh and rehydrated samples, the freezing temperature might not influence MSC-EVs lyophilized with 100 mM of trehalose. The reason why the effects caused by freezing at different temperatures is not observed is due to trehalose negating all the freezing stresses stated in section 2.11, by preventing ice crystal formation and incorporating into the membrane [209].

4.2.4 Total Protein Concentration of Lyophilized MSC-EVs Frozen at Different Temperatures

To determine whether freeze-drying MSC-EVs at different temperatures with 100 mM of trehalose affects protein concentration, a microBCA assay was performed once the EVs were rehydrated with results seen in Figure 17.

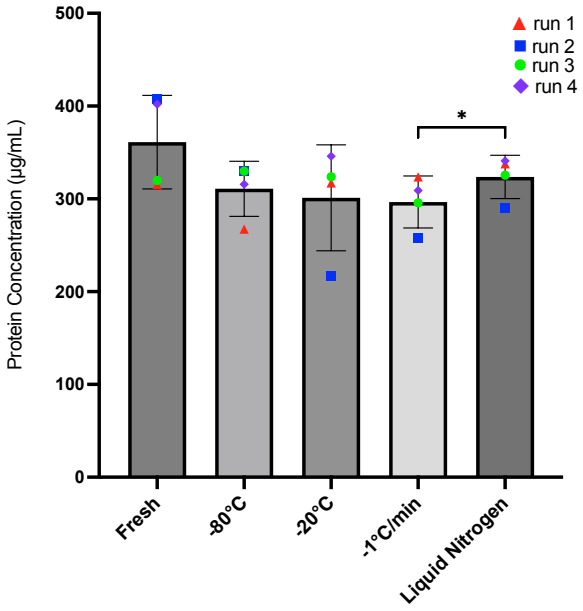

Figure 17. The total protein concentration (µg/mL) of fresh MSC-EVs and rehydrated MSC-EVs frozen at different temperatures determined by a microBCA assay. A one-way ANOVA followed by a Tukey multiple comparison test was used for statistical analysis. Values are presented as mean ± SD; n = 4. *p<0.05.

The total protein concentration of the fresh sample was 361.20 ± 50.39 µg/mL, while all rehydrated samples have a mean protein concentration that is lower than fresh MSC-EV but not low enough to claim that the different freezing temperatures affect protein concentration when compared to the fresh sample. The only significant difference observed was between -1°C/min and the liquid nitrogen sample (p-value: 0.0321), which could be due to the way these freezing conditions effect these aqueous solutions. This further suggests that when 100 mM of trehalose is added it protects the proteins from degradation that would occur by freezing at a slower or faster rates.

4.2.5 Morphology of MSC-EVs Freeze-Dried at Different Temperatures

To determine if freeze-drying at different temperatures effects the structural integrity of rehydrated MSC-EVs, TEM images were taken and displayed in Figure 18.

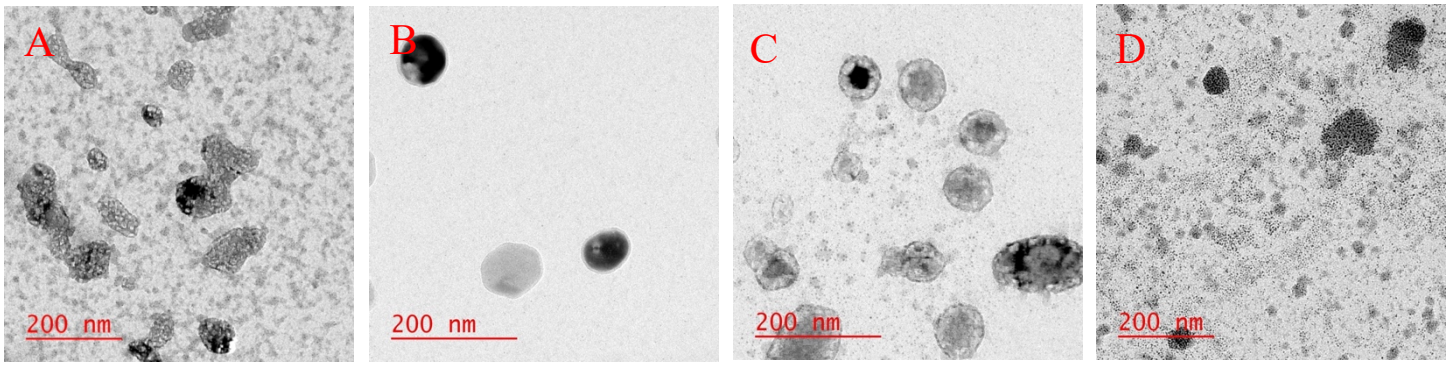

Figure 18. TEM images of rehydrated MSC-EVs that were freeze-dried at a temperature of (A) -1°C/min, (B) -20°C, (C) -80°C, or (D) -196°C.

From the TEM images we can confirm that the spherical shape, membrane integrity, and the size of MSC-EVs are all intact no matter what condition they were frozen at. Further affirming that as long as 100 mM of trehalose is present, freeze-drying MSC-EVs no matter the condition will not affect them.

These results show that when MSC-EVs are frozen at different temperatures with 100 mM of trehalose and then dried, the different freezing rates do not affect the structural characteristics of EVs and their protein concentration. The only significant difference observed between fresh, and the rehydrated sample was their particle size (Figure 15). When comparing the size distribution between the fresh and all the rehydrated sample there is a very clear shift in the peak size. However, when comparing the particle concentration and protein concentration there is no significant difference between the fresh and rehydrated samples. This suggests that different freezing temperature do not negatively affect the freezing drying processes once 100 mM of trehalose is added. Moreover, from the TEM images the structural integrity of the rehydrated MSC-EVs were maintained no matter the freezing temperature. These results show that once 100 mM of trehalose

is added, the protective capabilities can negate the affects different freezing temperature would have had. As a result, the deciding factor when choosing the optimum freeze temperature is convenience. Freezing a large amount of MSC-EVs at -1^{o}C/min requires building an apparatus that will maintain this temperature rate; while, freezing with liquid nitrogen will be costly. The best options are then -20^{o}C or -80^{o}C. Therefore, -20^{o}C was chosen as the ideal freezing temperature since it is the simplest temperature to reach and maintain.

The bioactive potential of the rehydrated MSC-EVs was tested by performing a tube formation assay, seen in Figure 19, followed by a NSPCs co-culture, seen in Figure 20.

4.3 Analyzing the angiogenic potential of rehydrated MSC-EVs via a tube formation assay

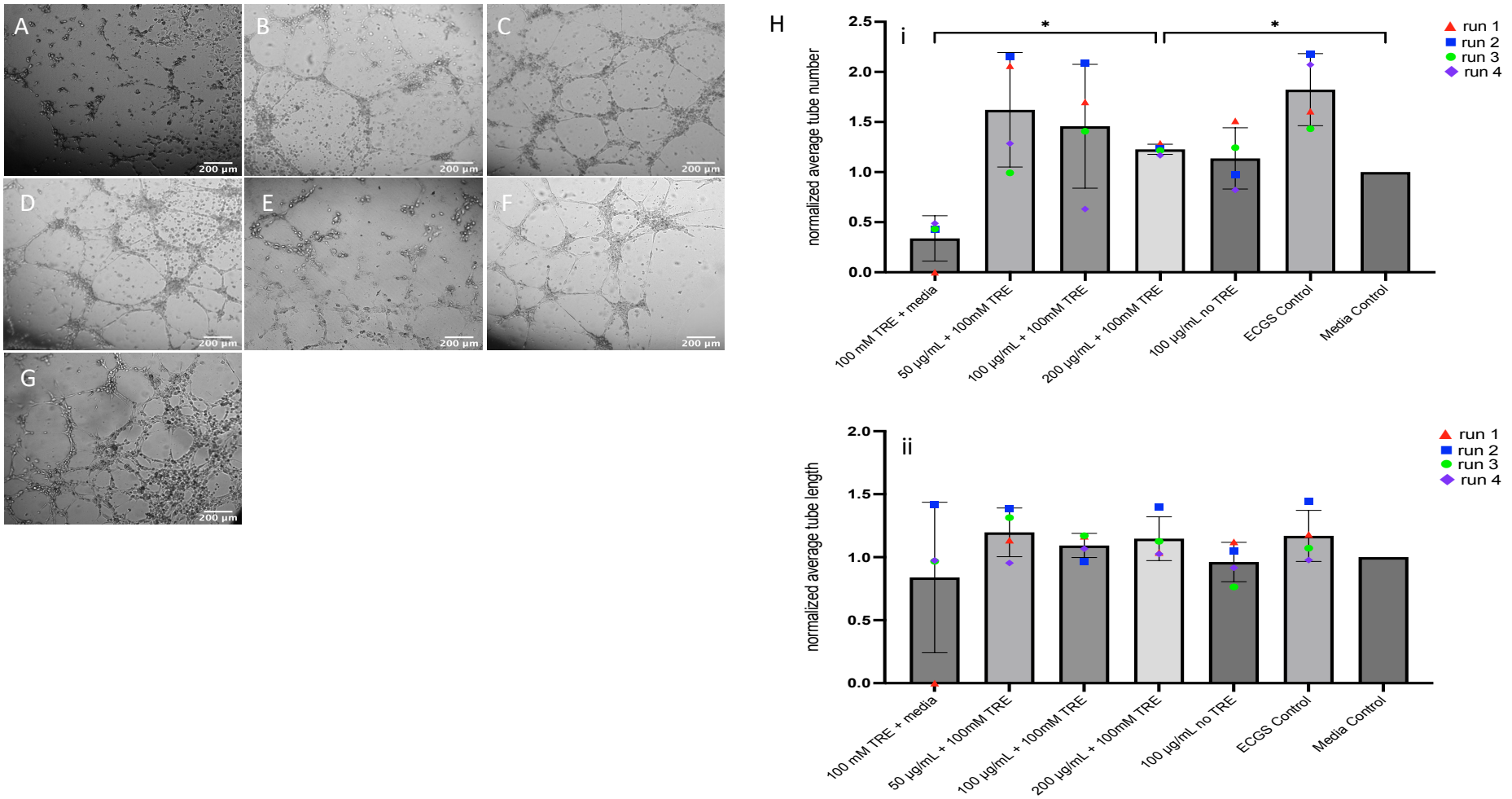

Figure 19. Tube formation assay to analyze the angiogenic capabilities of rehydrated MSC-EVs, freeze dried at the optimum conditions, at different total protein concentrations. (A) 0 µg/mL of MSC-EV protein, (B) 50 µg/mL of total MSC-EV protein, (C) 100 µg/mL of total MSC-EV protein, (D) 200 µg/mL of total MSC-EV protein, (E) 100 µg/mL of total MSC-EV protein freeze dried without trehalose, (F) ECGS control, (G) Media Control, and (H) quantitative analysis of the tube formation assay: (i) normalized number of tube formed, and (ii) normalized Average tube length. A one-way ANOVA followed by a Tukey multiple comparison test was used for statistical analysis. Data presented as mean ± SD, n = 4, *$p<0.05$).

A tube formation assay is a model used to identify stages of angiogenesis. The basis of this assay is to evaluate the ability of endothelial cells to form capillary-like structures, known as tubes, while platted on an extracellular matrix (ECM) support. It is a quantitative method to determine if a substrate can induce or inhibit tube formation. Once the endothelial attach to the ECM they produce a mechanical force to form pathways that support cellular migration to shape hollow lumen. In this study, a tube formation assay was used to assess if rehydrated MSC-EVs still retain their angiogenetic capabilities post freeze-drying and storage. As seen in Figure 19, all HUVECs treated with rehydrated MSC-EVs, even the MSC-EVs not protected by trehalose, exhibited tube formation. This is most likely due to the abundant amount of growth factors found in MSC-EVs such as, VEGF, PDGF [59], [123], miR-30b [123], and miR-125a [122]. The 200 μg/mL + 100mM TRE sample was significantly different than the 100mM TRE + media and the media control (p-values: 0.0394 and 0.0162, respectively). This is consistent with what has been reported in literature, where Gangadaran *et al*. had performed a tube formation assay by treating HUVECs with an increasing amount of fresh MSC-EV and reported that their lowest dosage was sufficient to induce a maximum response [118]. However, this same publication also states that fresh MSC-EVs caused at least 3-fold increases in tube formation and length, while our rehydrated MSC-EVs does not even induce a 2-fold increase. The reduced angiogenic potential of our rehydrated MSC-EVs could be due to the presence of trehalose. Even though trehalose is known to be an amazing cryoprotectant, Takeuchi *et al*. has reported that culturing HUVECs with trehalose downregulates VEGF receptor-2 (VEGFR2) production leading to a lack of angiogenesis [215]. This can also explain why very little to no tubes are formed when HUVECs are treated with just 100mM of trehalose. As for the HUVECs treated with rehydrated MSC-EVs that were not protected by trehalose, it was expected that the freeze-drying process would rupture a majority of the MSC-EVs

and irreversibly denature the growth factors but some MSC-EVs would survive. Therefore, tube formation was anticipated but at a lower level when compared to treatments with trehalose protected MSC-EVs. However, all MSC-EV treatments experienced the same fold increase, which can also be accounted for by the presence of trehalose reducing the efficacy of the MSC-EVs resulting in similar fold increases.

4.4 Analyzing the cellular proliferating capabilities of rehydrated MSC-EVs by co-culturing them with primary NSPCs

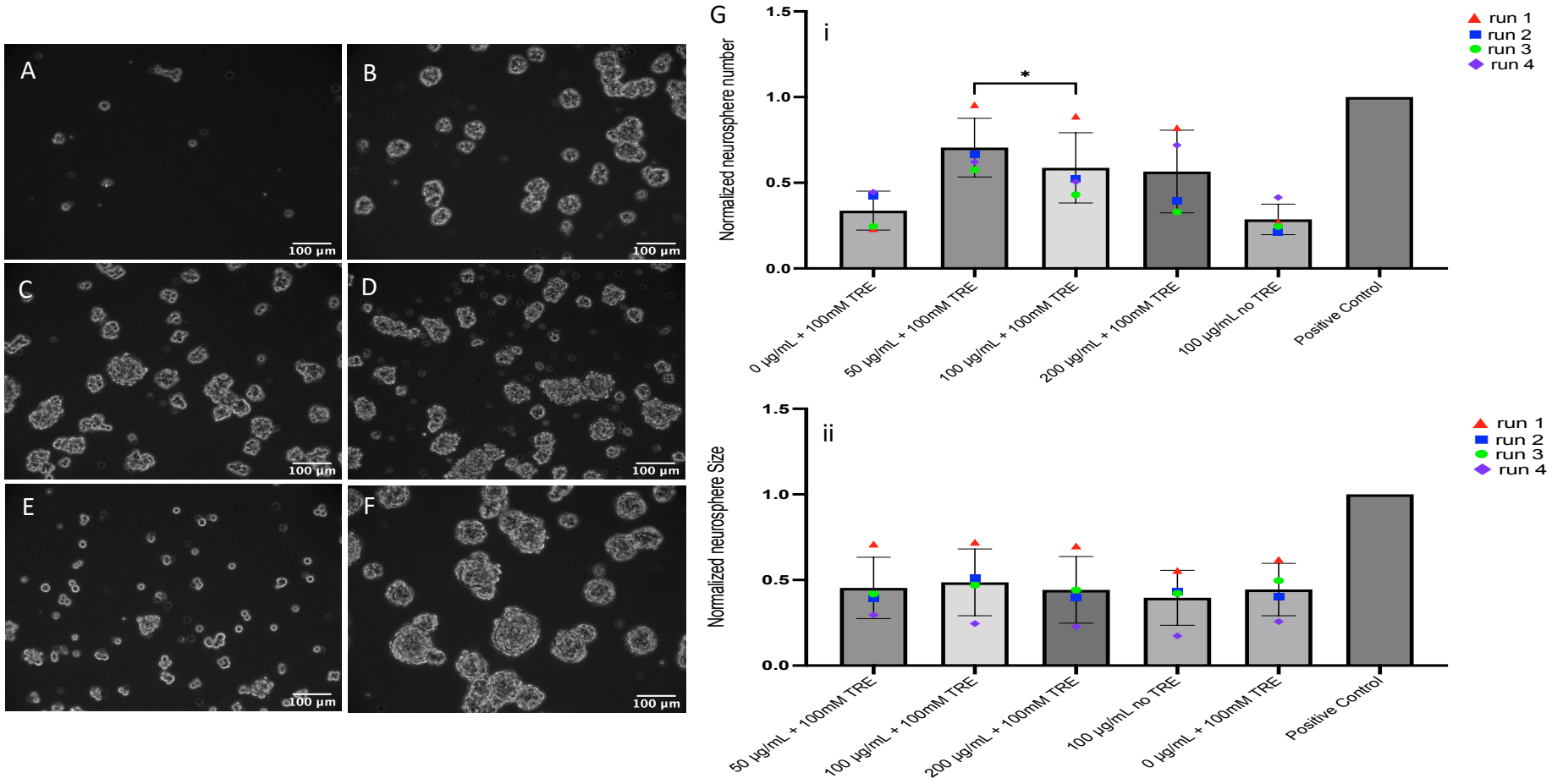

Figure 20. NSPC co-culture with rehydrated MSC-EVs, freeze dried at the optimum conditions, at different total protein concentrations. (A) 0 µg/mL of MSC-EV protein, (B) 50 µg/mL of total MSC-EV protein, (C) 100 µg/mL of total MSC-EV protein, (D) 200 µg/mL of total MSC-EV protein, (E) 100 µg/mL of total MSC-EV protein freeze dried without trehalose, (F) 20 ng/mL FGF2 and 20 ng/mL of EGF, and (G) quantitative analysis of co-culture: (i) normalized total number of NSPCs formed, and (ii) normalized average NSPC size. (A one-way ANOVA followed by a Tukey multiple comparison test was used for statistical analysis. Data presented as mean ± SD, n = 4, *$p<0.05$)

To further assess the bioactivity of rehydrated MSC-EVs, they were co-cultured, at different total protein concentrations, with NSPCs derived from the subventricular zone (SVZ) of rodent brains. As shown in Figure 20, NSPCs proliferated when treated with rehydrated MSC-EVs, with total protein concentrations of 50 µg/mL + 100mM (Figure 20B), 100 µg/mL + 100mM (Figure 20C), and 200 µg/mL + 100mM (Figure 20D), with no significant difference when compared to the positive control for both total number of NSPCs and for their average diameter. The formation of NSPCs could be due to biological factors found in MSC-EVs such as, BDNF, VEGF, and PDGF [57], [114]. These factors are not limited to proteins and can include microRNA such as, miR-124 [62], miR-184 [59], miR-133b [63], and miR cluster 17-92 [64]. The only significant difference observed was when comparing the normalized total number of NSPCs from the 50 ug/mL + 100mM TRE treatment to the 100ug/mL + 100mM TRE treatment (p-value: 0.036).

In the absences of MSC-EVs, and only containing 100 mM of trehalose, no NSPCs formed due to the lack of bioactive molecules and suggesting that trehalose does not promote NSPC proliferation. However, when treating NSPCs with rehydrated MSC-EVs that where not protected by trehalose, NSPCs where still present with very few new ones forming. This suggests that some of the bioactive molecules associated with NSPCs proliferation and growth become irreversibly damaged during the freeze-drying process.

To ensure the NSPCs treated with rehydrated MSC-EVs were multipotent, they were transferred to an adherent surface and allowed to differentiate in the presence of 10% FBS for one week. To assess that the NSPCs treated with rehydrated MSC-EVs are capable to differentiate into three main lineages of the CNS: oligodendrocytes, astrocytes, and neurons, immunostaining was utilized. As seen in Figure 21, Cells were stained positive for: O4 for oligodendrocytes (red),

GFAP for astrocytes (orange), and βIII-tubulin for neurons (green). Cells of all three linages were observed for all NSPCs treated with rehydrated MSC-EVs protected by trehalose.

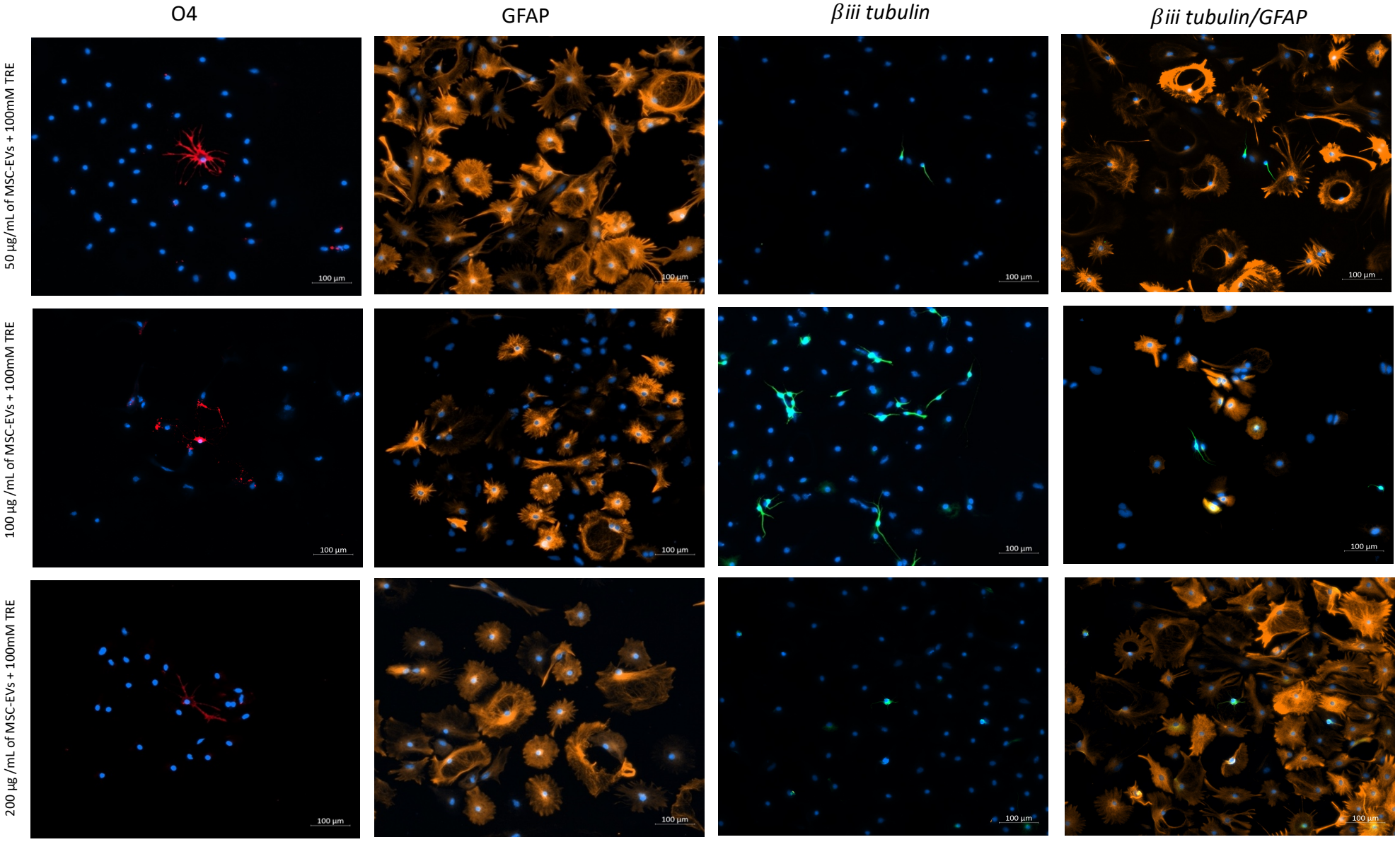
O4
GFAP
βiii tubulin
βiii tubulin/GFAP
50 µg/mL of MSC-EVs + 100mM TRE
100 µg /mL of MSC-EVs + 100mM TRE
200 µg /mL of MSC-EVs + 100mM TRE
100 µm

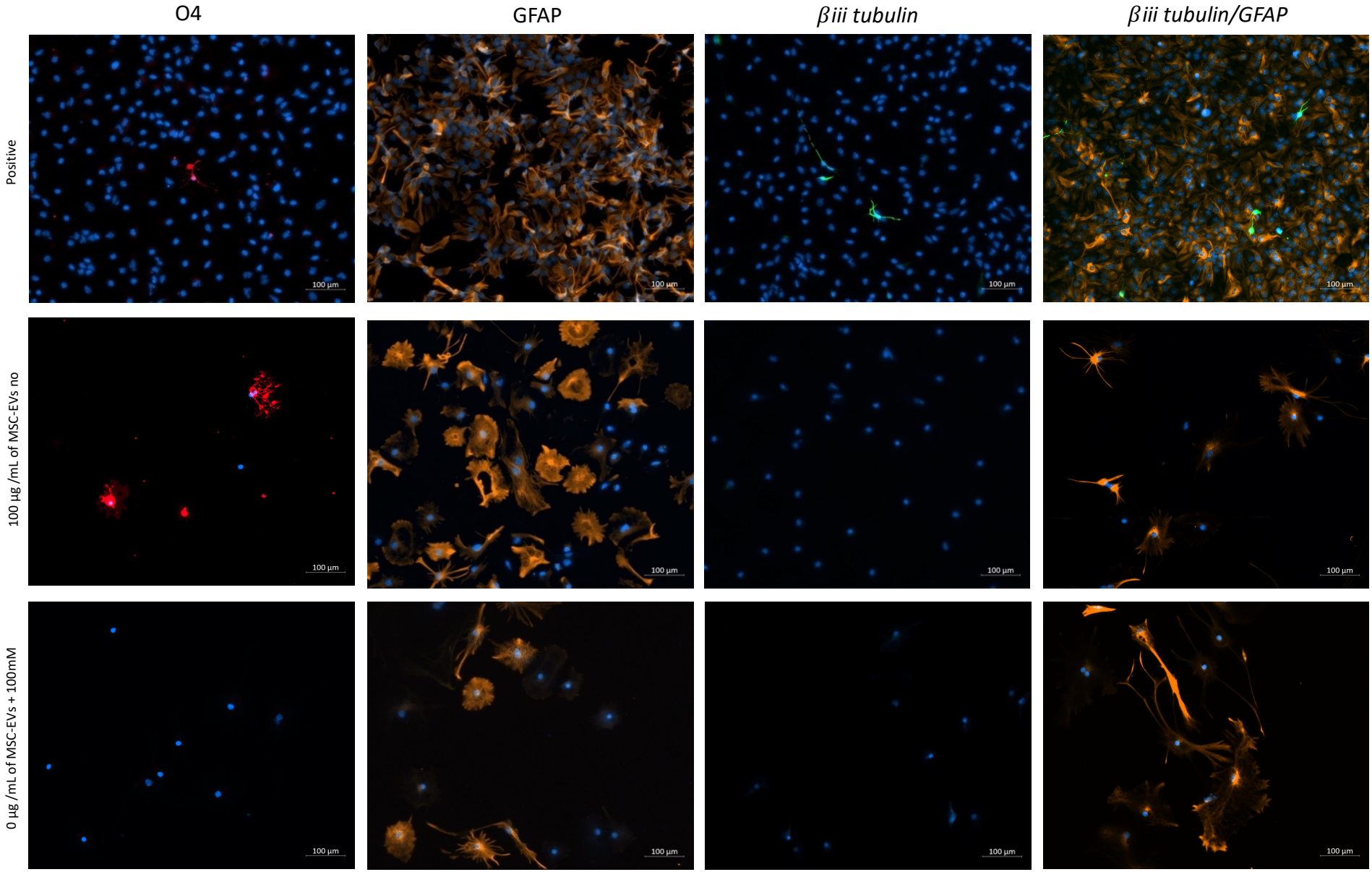

Figure 21. NSPCs were co-cultured with varying concentrations of rehydrated MSC-EVs and then left to differentiate in 10% FBS media for one week. O4 (red) is expressed on the surface of oligodendrocytes, GFAP (orange) is expressed in the cytoskeleton of astrocytes, and βIII-tubulin (green) is expressed on the cytoskeleton of neurons. All nuclei were counter stained with Hoechst (blue).

We further compared the expression levels of each differentiated cell type between the NSPCs treated with MSC-EVs to the positive control, as seen in Figure 22. We found that there was no significant difference between them no matter the concentration of MSC-EVs. Furthermore, the differentiated NSPCs preferred astrogenesis, over neurogenesis and ogliodendrogenesis. All in all, the freeze dried MSC-EVs did not affect the differentiating capabilities of NSPCs *in vitro*. Interestingly enough no neurons formed from the NSPCs treated with MSC-EVs that where not protected by trehalose during freeze drying.

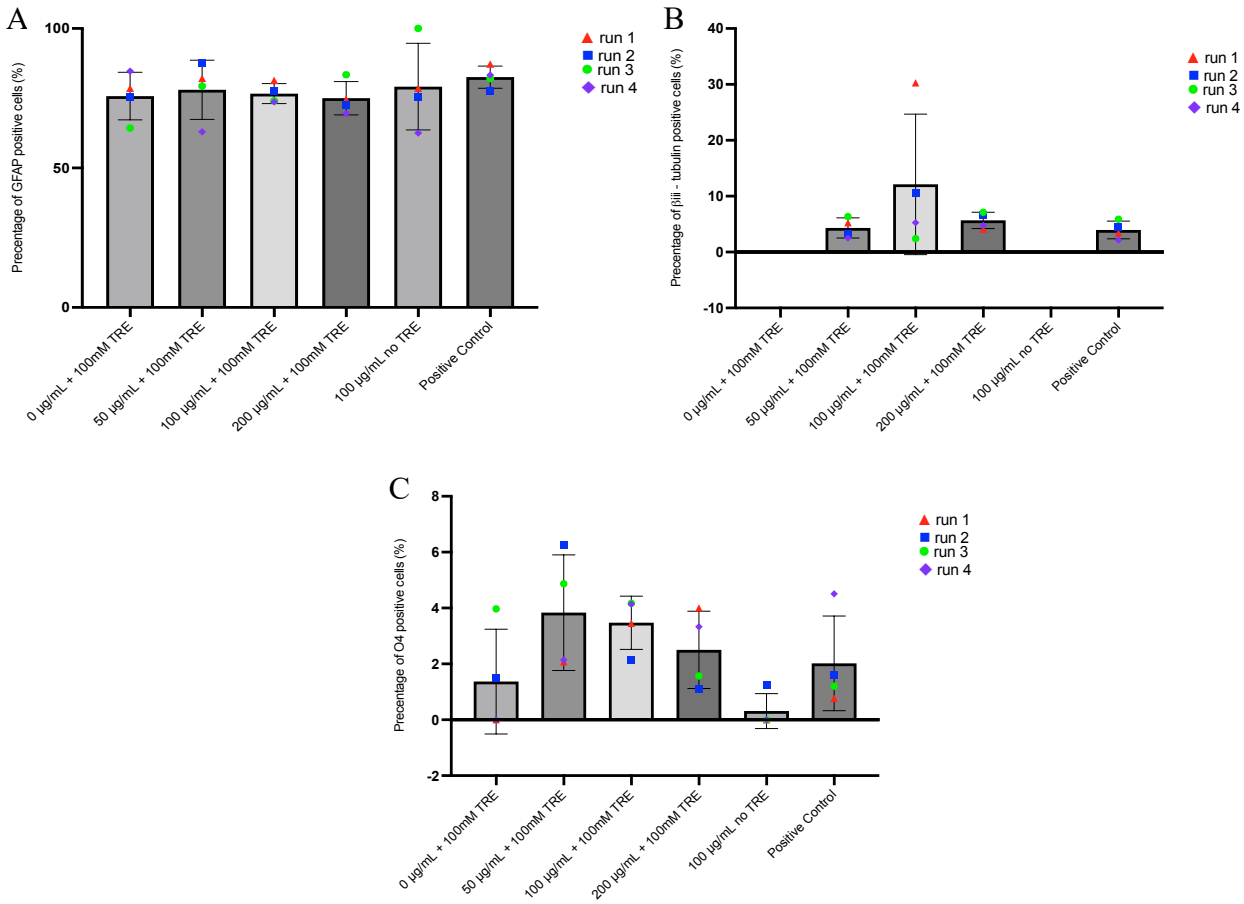

Figure 22. Expression levels of stained cells. Expression levels of O4 positive cells, Expression levels of GFAP positive cells, and Expression levels of βIII-tubulin positive cells. A one-way ANOVA followed by a Tukey multiple comparison test was used for statistical analysis. Data presented as mean ± SD, n = 4.

5 Conclusion

We determined the optimum freeze-drying conditions for MSC-EVs allowing them to be stored at room temperature for a long period of time while reducing aggregation and retaining their angiogenic and NSPC proliferation capabilities. By first lyophilizing the MSC-EVs in the presence of increasing trehalose concentration, 0 mM to 200 mM, we determined that concentrations greater than 100 mM, a narrower size distribution was observed indicating reduced aggregation, with no significant difference in protein and particle concentration when compared to fresh MSC-EVs. Then maintaining the trehalose concentration at 100mM, we froze the MSC-EVs at different freezing conditions, -20ºC, -80ºC, -1ºC/min, and -196ºC, to establish the optimum freezing temperature. We observed that in the presence of 100 mM of trehalose, none of the freezing conditions have a significant benefit or disadvantage over another. Therefore, the optimum conditions for freeze-drying MSC-EVs were found to be 100mM of trehalose and freezing at -20ºC. MSC-EVs lyophilized at these conditions where then rehydrated and showed that they can still promote cellular growth and proliferation via performing a tube formation assay and co-culturing them with NSPCs. We also observed that the rehydrated MSC-EVs did not affect the NSPCs ability to differentiate into oligodendrocytes, astrocytes, and neurons when cultured together.

6 Future Work

The next step for this project is incorporating the freeze-dried MSC-EVs into our cellulose based duraplasty, performing an MSC-EV release study, and then carrying out a decompressive craniectomy on MCAO stroked rats to observe any functional recovery by implanting the MSC-EV loaded duraplasty. However, a few improvements can be made to further optimize the freeze-drying process leading to a better MSC-EV product. For instance, trehalose is known to be a non-diffusing sugar and cannot pass through the plasma membrane, but studies have shown when

trehalose enters the cytosol, cryopreservation of cells is significantly improved. Therefore, getting trehalose into MSC-EVs could increase recovery and the methods to get trehalose past the membrane include electroporation, nano-injections, engineered transmembrane channels/pores, or ultrasound. To enhance the quality of the freeze-dried product, controlled ice crystal formation could be implemented during the freezing step. Currently, we are freezing our samples at -80^{o}C without introducing any ice crystals leading to random crystal formation, or random nucleation, causing inconsistent freezing among a batch of samples and introducing complications during primary drying, all resulting in a lower quality product. To avoid this force/controlled nucleation is utilized which introduces small ice crystals into every sample resulting in consistent crystal formation amongst a batch of samples ensuring a higher quality product post lyophilization. To further refine the drying process an updated lyophilizer should be used. At this time, our freeze-dyer does not allow us to control the temperature causing both drying phases to occur at room temperature. However, to drop the water content to 1% during the secondary drying phase the temperature should increase to help break the interactions between bound water and the MSC-EVs. Updated freeze-dryers can control the temperature of the sample during all stages of drying ensuring the temperature during secondary drying is higher than the temperature during primary drying allowing for optimum drying.

7 References

[1] J. Doorn, G. Moll, K. Le Blanc, C. van Blitterswijk, and J. de Boer, "Therapeutic Applications of Mesenchymal Stromal Cells: Paracrine Effects and Potential Improvements," *Tissue Engineering Part B: Reviews*, vol. 18, no. 2, pp. 101–115, Oct. 2011, doi: 10.1089/ten.teb.2011.0488.

[2] B. G. Stultz, K. McGinnis, E. E. Thompson, J. L. Lo Surdo, S. R. Bauer, and D. A. Hursh, "Chromosomal stability of mesenchymal stromal cells during in vitro culture," *Cytotherapy*, vol. 18, no. 3, pp. 336–343, Mar. 2016, doi: 10.1016/j.jcyt.2015.11.017.

[3] S. Schrepfer, T. Deuse, H. Reichenspurner, M. P. Fischbein, R. C. Robbins, and M. P. Pelletier, "Stem Cell Transplantation: The Lung Barrier," *Transplantation Proceedings*, vol. 39, no. 2, pp. 573–576, Mar. 2007, doi: 10.1016/j.transproceed.2006.12.019.

[4] J. A. Pawitan, "Prospect of stem cell conditioned medium in regenerative medicine," *BioMed research international*, vol. 2014, 2014.

[5] A. Jeyaram and S. M. Jay, "Preservation and storage stability of extracellular vesicles for therapeutic applications," *The AAPS journal*, vol. 20, no. 1, pp. 1–7, 2018.

[6] G. D. Kusuma, M. Barabadi, J. L. Tan, D. A. Morton, J. E. Frith, and R. Lim, "To protect and to preserve: novel preservation strategies for extracellular vesicles," *Frontiers in Pharmacology*, vol. 9, p. 1199, 2018.

[7] D. Mozaffarian *et al.*, "Heart disease and stroke statistics—2016 update: a report from the American Heart Association," *circulation*, vol. 133, no. 4, pp. e38–e360, 2016.

[8] G. H. Estimates, "Disease burden by Cause, Age, Sex, by Country and by Region, 2000-2015," *Geneva: World Health Organization*, 2016.

[9] World Health Organization, "Global health estimates 2015: Disease burden by cause, age, sex, by country and by region, 2000–2015," *Geneva: World Health Organization*, 2016.

[10] P. H. A. of Canada, "Stroke in Canada," Oct. 27, 2016. https://www.canada.ca/en/public-health/services/publications/diseases-conditions/stroke-in-canada.html (accessed Jun. 29, 2022).

[11] P. Sensharma, G. Madhumathi, R. D. Jayant, and A. K. Jaiswal, "Biomaterials and cells for neural tissue engineering: Current choices," *Materials Science and Engineering: C*, vol. 77, pp. 1302–1315, 2017.

[12] M. Fisher, A. Dávalos, A. Rogalewski, A. Schneider, E. B. Ringelstein, and W.-R. Schäbitz, "Toward a multimodal neuroprotective treatment of stroke," *Stroke*, vol. 37, no. 4, pp. 1129–1136, 2006.

[13] R. Y. Tam, T. Fuehrmann, N. Mitrousis, and M. S. Shoichet, "Regenerative therapies for central nervous system diseases: a biomaterials approach," *Neuropsychopharmacology*, vol. 39, no. 1, pp. 169–188, 2014.

[14] Staykov Dimitre and Gupta Rishi, "Hemicraniectomy in Malignant Middle Cerebral Artery Infarction," *Stroke*, vol. 42, no. 2, pp. 513–516, Feb. 2011, doi: 10.1161/STROKEAHA.110.605642.

[15] O. M. Arnaout, S. G. Aoun, H. H. Batjer, and B. R. Bendok, "Decompressive hemicraniectomy after malignant middle cerebral artery infarction: rationale and controversies," *Neurosurgical focus*, vol. 30, no. 6, p. E18, 2011.

[16] E. Jüttler *et al.*, "Hemicraniectomy in Older Patients with Extensive Middle-Cerebral-Artery Stroke," *New England Journal of Medicine*, vol. 370, no. 12, pp. 1091–1100, Mar. 2014, doi: 10.1056/NEJMoa1311367.

[17] X. Lu *et al.*, "Decompressive craniectomy for the treatment of malignant infarction of the middle cerebral artery," *Scientific reports*, vol. 4, no. 1, pp. 1–9, 2014.
[18] T. R. Stumpf *et al.*, "Design and evaluation of a biosynthesized cellulose drug releasing duraplasty," *Materials Science and Engineering: C*, vol. 110, p. 110677, May 2020, doi: 10.1016/j.msec.2020.110677.
[19] L. Biancone, S. Bruno, M. C. Deregibus, C. Tetta, and G. Camussi, "Therapeutic potential of mesenchymal stem cell-derived microvesicles," *Nephrology Dialysis Transplantation*, vol. 27, no. 8, pp. 3037–3042, Aug. 2012, doi: 10.1093/ndt/gfs168.
[20] T. Katsuda, N. Kosaka, F. Takeshita, and T. Ochiya, "The therapeutic potential of mesenchymal stem cell-derived extracellular vesicles," *PROTEOMICS*, vol. 13, no. 10–11, pp. 1637–1653, 2013, doi: https://doi.org/10.1002/pmic.201200373.
[21] W. S. Toh, R. C. Lai, B. Zhang, and S. K. Lim, "MSC exosome works through a protein-based mechanism of action," *Biochemical Society Transactions*, vol. 46, no. 4, pp. 843–853, 2018.
[22] A. B. Nair and S. Jacob, "A simple practice guide for dose conversion between animals and human," *J Basic Clin Pharm*, vol. 7, no. 2, pp. 27–31, Mar. 2016, doi: 10.4103/0976-0105.177703.
[23] E. D. Sverdlov, "Amedeo Avogadro's cry: What is 1 μg of exosomes?," *BioEssays*, vol. 34, no. 10, pp. 873–875, 2012, doi: 10.1002/bies.201200045.
[24] M. Record, C. Subra, S. Silvente-Poirot, and M. Poirot, "Exosomes as intercellular signalosomes and pharmacological effectors," *Biochemical Pharmacology*, vol. 81, no. 10, pp. 1171–1182, May 2011, doi: 10.1016/j.bcp.2011.02.011.
[25] E. G. Evtushenko, D. V. Bagrov, V. N. Lazarev, M. A. Livshits, and E. Khomyakova, "Adsorption of extracellular vesicles onto the tube walls during storage in solution," *PloS one*, vol. 15, no. 12, p. e0243738, 2020.
[26] S. Jiang and S. L. Nail, "Effect of process conditions on recovery of protein activity after freezing and freeze-drying," *European Journal of Pharmaceutics and Biopharmaceutics*, vol. 45, no. 3, pp. 249–257, 1998.
[27] J. Frank, M. Richter, C. de Rossi, C.-M. Lehr, K. Fuhrmann, and G. Fuhrmann, "Extracellular vesicles protect glucuronidase model enzymes during freeze-drying," *Scientific Reports*, vol. 8, no. 1, Art. no. 1, Aug. 2018, doi: 10.1038/s41598-018-30786-y.
[28] C. Colaco, S. Sen, M. Thangavelu, S. Pinder, and B. Roser, "Extraordinary stability of enzymes dried in trehalose: simplified molecular biology," *Bio/technology*, vol. 10, no. 9, pp. 1007–1011, 1992.
[29] K. B. Y. El Baradie *et al.*, "Freeze-Dried Extracellular Vesicles From Adipose-Derived Stem Cells Prevent Hypoxia-Induced Muscle Cell Injury," *Front. Cell Dev. Biol.*, vol. 8, 2020, doi: 10.3389/fcell.2020.00181.
[30] E. Trenkenschuh, M. Richter, E. Heinrich, M. Koch, G. Fuhrmann, and W. Friess, "Enhancing the Stabilization Potential of Lyophilization for Extracellular Vesicles," *Advanced Healthcare Materials*, vol. 11, no. 5, p. 2100538, 2022, doi: 10.1002/adhm.202100538.
[31] M. Guarro, F. Suñer, M. Lecina, S. Borrós, and C. Fornaguera, "Efficient extracellular vesicles freeze-dry method for direct formulations preparation and use," *Colloids and Surfaces B: Biointerfaces*, vol. 218, p. 112745, Oct. 2022, doi: 10.1016/j.colsurfb.2022.112745.

[32] Y. Wang, H. Tan, and X. Hui, “Biomaterial scaffolds in regenerative therapy of the central nervous system,” *BioMed research international*, vol. 2018, 2018.
[33] M. T. Fitch and J. Silver, “CNS injury, glial scars, and inflammation: Inhibitory extracellular matrices and regeneration failure,” *Experimental neurology*, vol. 209, no. 2, pp. 294–301, 2008.
[34] P. Dibajnia and C. M. Morshead, “Role of neural precursor cells in promoting repair following stroke,” *Acta Pharmacologica Sinica*, vol. 34, no. 1, pp. 78–90, 2013.
[35] C.-T. Lu, Y.-Z. Zhao, H. L. Wong, J. Cai, L. Peng, and X.-Q. Tian, “Current approaches to enhance CNS delivery of drugs across the brain barriers,” *International journal of nanomedicine*, vol. 9, p. 2241, 2014.
[36] J. Brownlees and C. Williams, “Peptidases, peptides, and the mammalian blood–brain barrier,” *Journal of neurochemistry*, vol. 60, no. 3, pp. 793–803, 1993.
[37] J. Wu, S.-H. Yoon, W.-M. Wu, and N. Bodor, “Synthesis and biological evaluations of brain-targeted chemical delivery systems of [Nva2]-TRH,” *Journal of pharmacy and pharmacology*, vol. 54, no. 7, pp. 945–950, 2002.
[38] P. P. Wang, J. Frazier, and H. Brem, “Local drug delivery to the brain,” *Advanced drug delivery reviews*, vol. 54, no. 7, pp. 987–1013, 2002.
[39] M. M. Pakulska, B. G. Ballios, and M. S. Shoichet, “Injectable hydrogels for central nervous system therapy,” *Biomedical materials*, vol. 7, no. 2, p. 024101, 2012.
[40] World Health Organization, “Global health estimates 2016: deaths by cause, age, sex, by country and by region, 2000–2016,” *Geneva: World Health Organization*, 2018.
[41] World Health Organization, “The atlas of heart disease and stroke,” World Health Organization, 2004. Accessed: Oct. 23, 2022. [Online]. Available: https://apps.who.int/iris/handle/10665/43007
[42] L.-P. Pallesen, K. Barlinn, and V. Puetz, “Role of Decompressive Craniectomy in Ischemic Stroke,” *Front. Neurol.*, vol. 9, 2019, doi: 10.3389/fneur.2018.01119.
[43] V. Pencea, K. D. Bingaman, L. J. Freedman, and M. B. Luskin, “Neurogenesis in the subventricular zone and rostral migratory stream of the neonatal and adult primate forebrain,” *Experimental neurology*, vol. 172, no. 1, pp. 1–16, 2001.
[44] S. G. Kernie and J. M. Parent, “Forebrain neurogenesis after focal Ischemic and traumatic brain injury,” *Neurobiology of disease*, vol. 37, no. 2, pp. 267–274, 2010.
[45] L. Li, K. M. Harms, P. B. Ventura, D. C. Lagace, A. J. Eisch, and L. A. Cunningham, “Focal cerebral ischemia induces a multilineage cytogenic response from adult subventricular zone that is predominantly gliogenic,” *Glia*, vol. 58, no. 13, pp. 1610–1619, 2010.
[46] T. Ikeda *et al.*, “Limited differentiation to neurons and astroglia from neural stem cells in the cortex and striatum after ischemia/hypoxia in the neonatal rat brain,” *American Journal of Obstetrics and Gynecology*, vol. 193, no. 3, pp. 849–856, Sep. 2005, doi: 10.1016/j.ajog.2005.01.029.
[47] J. Lu, A. Manaenko, and Q. Hu, “Targeting adult neurogenesis for poststroke therapy,” *Stem Cells International*, vol. 2017, 2017.
[48] R. J. Felling and S. W. Levison, “Enhanced neurogenesis following stroke,” *Journal of neuroscience research*, vol. 73, no. 3, pp. 277–283, 2003.
[49] K. Jin *et al.*, “Evidence for stroke-induced neurogenesis in the human brain,” *Proceedings of the National Academy of Sciences*, vol. 103, no. 35, pp. 13198–13202, 2006.

[50] A. Arvidsson, T. Collin, D. Kirik, Z. Kokaia, and O. Lindvall, "Neuronal replacement from endogenous precursors in the adult brain after stroke," *Nature medicine*, vol. 8, no. 9, pp. 963–970, 2002.
[51] K. Wada, H. Sugimori, P. G. Bhide, M. A. Moskowitz, and S. P. Finklestein, "Effect of basic fibroblast growth factor treatment on brain progenitor cells after permanent focal ischemia in rats," *Stroke*, vol. 34, no. 11, pp. 2722–2728, 2003.
[52] T. Kawamata, J. Ren, T. C. Chan, M. Charette, and S. P. Finklestein, "Intracisternal osteogenic protein-1 enhances functional recovery following focal stroke," *Neuroreport*, vol. 9, no. 7, pp. 1441–1445, 1998.
[53] T. Hayashi, K. Abe, and Y. Itoyama, "Reduction of ischemic damage by application of vascular endothelial growth factor in rat brain after transient ischemia," *Journal of Cerebral Blood Flow & Metabolism*, vol. 18, no. 8, pp. 887–895, 1998.
[54] Y. Sun, "Jin K, Xie L, Childs J, Mao XO, Logvinova A, Greenberg DA," *VEGF-induced neuroprotection, neurogenesis, and angiogenesis after focal cerebral ischemia. J Clin Invest*, vol. 111, pp. 1843–1851, 2003.
[55] L. Wang, Z. Zhang, Y. Wang, R. Zhang, and M. Chopp, "Treatment of stroke with erythropoietin enhances neurogenesis and angiogenesis and improves neurological function in rats," *Stroke*, vol. 35, no. 7, pp. 1732–1737, 2004.
[56] R. Böttger, R. Hoffmann, and D. Knappe, "Differential stability of therapeutic peptides with different proteolytic cleavage sites in blood, plasma and serum," *PloS one*, vol. 12, no. 6, p. e0178943, 2017.
[57] J. Chen *et al.*, "Hypoxic Preconditioning Augments the Therapeutic Efficacy of Bone Marrow Stromal Cells in a Rat Ischemic Stroke Model," *Cell Mol Neurobiol*, vol. 37, no. 6, pp. 1115–1129, Aug. 2017, doi: 10.1007/s10571-016-0445-1.
[58] T. R. Doeppner *et al.*, "Extracellular Vesicles Improve Post-Stroke Neuroregeneration and Prevent Postischemic Immunosuppression," *STEM CELLS Translational Medicine*, vol. 4, no. 10, pp. 1131–1143, 2015, doi: 10.5966/sctm.2015-0078.
[59] G. J. Moon *et al.*, "Application of Mesenchymal Stem Cell-Derived Extracellular Vesicles for Stroke: Biodistribution and MicroRNA Study," *Transl. Stroke Res.*, vol. 10, no. 5, pp. 509–521, Oct. 2019, doi: 10.1007/s12975-018-0668-1.
[60] S.-Y. Chen *et al.*, "EP4 Antagonist-Elicited Extracellular Vesicles from Mesenchymal Stem Cells Rescue Cognition/Learning Deficiencies by Restoring Brain Cellular Functions," *STEM CELLS Translational Medicine*, vol. 8, no. 7, pp. 707–723, 2019, doi: 10.1002/sctm.18-0284.
[61] J. Wang, L. Yin, and Z. Chen, "Neuroprotective role of fibronectin in neuron-glial extrasynaptic transmission," *Neural regeneration research*, vol. 8, no. 4, p. 376, 2013.
[62] J. Yang, X. Zhang, X. Chen, L. Wang, and G. Yang, "Exosome Mediated Delivery of miR-124 Promotes Neurogenesis after Ischemia," *Molecular Therapy - Nucleic Acids*, vol. 7, pp. 278–287, Jun. 2017, doi: 10.1016/j.omtn.2017.04.010.
[63] H. Xin *et al.*, "Exosome-Mediated Transfer of miR-133b from Multipotent Mesenchymal Stromal Cells to Neural Cells Contributes to Neurite Outgrowth," *STEM CELLS*, vol. 30, no. 7, pp. 1556–1564, 2012, doi: 10.1002/stem.1129.
[64] Xin Hongqi *et al.*, "MicroRNA-17–92 Cluster in Exosomes Enhance Neuroplasticity and Functional Recovery After Stroke in Rats," *Stroke*, vol. 48, no. 3, pp. 747–753, Mar. 2017, doi: 10.1161/STROKEAHA.116.015204.

[65] S.-C. Tao, T. Yuan, Y.-L. Zhang, W.-J. Yin, S.-C. Guo, and C.-Q. Zhang, "Exosomes derived from miR-140-5p-overexpressing human synovial mesenchymal stem cells enhance cartilage tissue regeneration and prevent osteoarthritis of the knee in a rat model," *Theranostics*, vol. 7, no. 1, p. 180, 2017.
[66] G. Ju *et al.*, "Microvesicles derived from human umbilical cord mesenchymal stem cells facilitate tubular epithelial cell dedifferentiation and growth via hepatocyte growth factor induction," *PloS one*, vol. 10, no. 3, p. e0121534, 2015.
[67] J. Ma *et al.*, "Exosomes Derived from Akt-Modified Human Umbilical Cord Mesenchymal Stem Cells Improve Cardiac Regeneration and Promote Angiogenesis via Activating Platelet-Derived Growth Factor D," *Stem Cells Translational Medicine*, vol. 6, no. 1, pp. 51–59, Jan. 2017, doi: 10.5966/sctm.2016-0038.
[68] R. Rahme *et al.*, "How often are patients with ischemic stroke eligible for decompressive hemicraniectomy?," *Stroke*, vol. 43, no. 2, pp. 550–552, 2012.
[69] K. Vahedi *et al.*, "Early decompressive surgery in malignant infarction of the middle cerebral artery: a pooled analysis of three randomised controlled trials," *The Lancet Neurology*, vol. 6, no. 3, pp. 215–222, 2007.
[70] M. Geurts, H. B. van der Worp, L. J. Kappelle, G. J. Amelink, A. Algra, and J. Hofmeijer, "Surgical decompression for space-occupying cerebral infarction: outcomes at 3 years in the randomized HAMLET trial," *Stroke*, vol. 44, no. 9, pp. 2506–2508, 2013.
[71] A. Friedenstein, R. Chailakhjan, and K. Lalykina, "The development of fibroblast colonies in monolayer cultures of guinea-pig bone marrow and spleen cells," *Cell Proliferation*, vol. 3, no. 4, pp. 393–403, 1970.
[72] T. Dexter, E. Wright, F. Krizsa, and L. Lajtha, "Regulation of haemopoietic stem cell proliferation in long term bone marrow cultures.," *Biomedicine/[publiee pour l'AAICIG]*, vol. 27, no. 9–10, pp. 344–349, 1977.
[73] J. R. Lavoie and M. Rosu-Myles, "Uncovering the secretes of mesenchymal stem cells," *Biochimie*, vol. 95, no. 12, pp. 2212–2221, 2013.
[74] M. Kim, I. E. Erickson, A. H. Huang, S. T. Garrity, R. L. Mauck, and D. R. Steinberg, "Donor variation and optimization of human mesenchymal stem cell chondrogenesis in hyaluronic acid," *Tissue Engineering Part A*, vol. 24, no. 21–22, pp. 1693–1703, 2018.
[75] I. Ullah, R. B. Subbarao, and G. J. Rho, "Human mesenchymal stem cells-current trends and future prospective," *Bioscience reports*, vol. 35, no. 2, 2015.
[76] S. Ma, N. Xie, W. Li, B. Yuan, Y. Shi, and Y. Wang, "Immunobiology of mesenchymal stem cells," *Cell Death & Differentiation*, vol. 21, no. 2, pp. 216–225, 2014.
[77] R. H. Lee *et al.*, "Intravenous hMSCs improve myocardial infarction in mice because cells embolized in lung are activated to secrete the anti-inflammatory protein TSG-6," *Cell stem cell*, vol. 5, no. 1, pp. 54–63, 2009.
[78] A. I. Caplan and D. Correa, "The MSC: an injury drugstore," *Cell stem cell*, vol. 9, no. 1, pp. 11–15, 2011.
[79] T. Lener *et al.*, "Applying extracellular vesicles based therapeutics in clinical trials–an ISEV position paper," *Journal of extracellular vesicles*, vol. 4, no. 1, p. 30087, 2015.
[80] L. Timmers *et al.*, "Reduction of myocardial infarct size by human mesenchymal stem cell conditioned medium," *Stem cell research*, vol. 1, no. 2, pp. 129–137, 2008.
[81] L. Timmers *et al.*, "Human mesenchymal stem cell-conditioned medium improves cardiac function following myocardial infarction," *Stem cell research*, vol. 6, no. 3, pp. 206–214, 2011.

[82] Z. Du *et al.*, “Mesenchymal stem cell–conditioned medium reduces liver injury and enhances regeneration in reduced-size rat liver transplantation,” *Journal of Surgical Research*, vol. 183, no. 2, pp. 907–915, 2013.
[83] D. S. Zagoura *et al.*, “Therapeutic potential of a distinct population of human amniotic fluid mesenchymal stem cells and their secreted molecules in mice with acute hepatic failure,” *Gut*, vol. 61, no. 6, pp. 894–906, 2012.
[84] D. Van Poll *et al.*, “Mesenchymal stem cell–derived molecules directly modulate hepatocellular death and regeneration in vitro and in vivo,” *Hepatology*, vol. 47, no. 5, pp. 1634–1643, 2008.
[85] B. Parekkadan *et al.*, “Mesenchymal stem cell-derived molecules reverse fulminant hepatic failure,” *PloS one*, vol. 2, no. 9, p. e941, 2007.
[86] T. Inoue, M. Sugiyama, H. Hattori, H. Wakita, T. Wakabayashi, and M. Ueda, “Stem cells from human exfoliated deciduous tooth-derived conditioned medium enhance recovery of focal cerebral ischemia in rats,” *Tissue Engineering Part A*, vol. 19, no. 1–2, pp. 24–29, 2013.
[87] Y. J. Cho *et al.*, “Therapeutic effects of human adipose stem cell-conditioned medium on stroke,” *Journal of neuroscience research*, vol. 90, no. 9, pp. 1794–1802, 2012.
[88] B. Bakondi *et al.*, “CD133 identifies a human bone marrow stem/progenitor cell sub-population with a repertoire of secreted factors that protect against stroke,” *Molecular Therapy*, vol. 17, no. 11, pp. 1938–1947, 2009.
[89] T.-J. Chuang, K.-C. Lin, C.-C. Chio, C.-C. Wang, C.-P. Chang, and J.-R. Kuo, “Effects of secretome obtained from normoxia-preconditioned human mesenchymal stem cells in traumatic brain injury rats,” *Journal of Trauma and Acute Care Surgery*, vol. 73, no. 5, pp. 1161–1167, 2012.
[90] C.-P. Chang, C.-C. Chio, C.-U. Cheong, C.-M. Chao, B.-C. Cheng, and M.-T. Lin, “Hypoxic preconditioning enhances the therapeutic potential of the secretome from cultured human mesenchymal stem cells in experimental traumatic brain injury,” *Clinical Science*, vol. 124, no. 3, pp. 165–176, 2013.
[91] D. Cantinieaux *et al.*, “Conditioned medium from bone marrow-derived mesenchymal stem cells improves recovery after spinal cord injury in rats: an original strategy to avoid cell transplantation,” *PloS one*, vol. 8, no. 8, p. e69515, 2013.
[92] A. van Koppen *et al.*, “Human embryonic mesenchymal stem cell-derived conditioned medium rescues kidney function in rats with established chronic kidney disease,” *PloS one*, vol. 7, no. 6, p. e38746, 2012.
[93] Y. Gheisari, N. Ahmadbeigi, M. Naderi, S. M. Nassiri, S. Nadri, and M. Soleimani, “Stem cell-conditioned medium does not protect against kidney failure,” *Cell biology international*, vol. 35, no. 3, pp. 209–213, 2011.
[94] M. Mouiseddine *et al.*, “Human mesenchymal stem cells home specifically to radiation-injured tissues in a non-obese diabetes/severe combined immunodeficiency mouse model,” *BJR*, vol. 80, no. special_issue_1, pp. S49–S55, Sep. 2007, doi: 10.1259/bjr/25927054.
[95] G. R. Willis, S. Kourembanas, and S. A. Mitsialis, “Toward Exosome-Based Therapeutics: Isolation, Heterogeneity, and Fit-for-Purpose Potency,” *Frontiers in Cardiovascular Medicine*, vol. 4, 2017, Accessed: Jun. 20, 2022. [Online]. Available: https://www.frontiersin.org/article/10.3389/fcvm.2017.00063

[96] Y.-S. Chen, E.-Y. Lin, T.-W. Chiou, and H.-J. Harn, "Exosomes in clinical trial and their production in compliance with good manufacturing practice," *Tzu-Chi Medical Journal*, vol. 32, no. 2, p. 113, 2020.
[97] R. J. Simpson, S. S. Jensen, and J. W. E. Lim, "Proteomic profiling of exosomes: Current perspectives," *PROTEOMICS*, vol. 8, no. 19, pp. 4083–4099, 2008, doi: 10.1002/pmic.200800109.
[98] B.-T. Pan and R. M. Johnstone, "Fate of the transferrin receptor during maturation of sheep reticulocytes in vitro: Selective externalization of the receptor," *Cell*, vol. 33, no. 3, pp. 967–978, Jul. 1983, doi: 10.1016/0092-8674(83)90040-5.
[99] R. M. Johnstone, "Revisiting the road to the discovery of exosomes," *Blood Cells, Molecules, and Diseases*, vol. 34, no. 3, pp. 214–219, May 2005, doi: 10.1016/j.bcmd.2005.03.002.
[100] C. Lawson, D. Kovacs, E. Finding, E. Ulfelder, and V. Luis-Fuentes, "Extracellular Vesicles: Evolutionarily Conserved Mediators of Intercellular Communication," *Yale J Biol Med*, vol. 90, no. 3, pp. 481–491, Sep. 2017.
[101] T. R. Doeppner, M. Bähr, D. M. Hermann, and B. Giebel, "Concise Review: Extracellular Vesicles Overcoming Limitations of Cell Therapies in Ischemic Stroke," *Stem Cells Translational Medicine*, vol. 6, no. 11, pp. 2044–2052, Nov. 2017, doi: 10.1002/sctm.17-0081.
[102] Y. Li *et al.*, "Extracellular vesicles in mesenchymal stromal cells: A novel therapeutic strategy for stroke (Review)," *Experimental and Therapeutic Medicine*, vol. 15, no. 5, pp. 4067–4079, May 2018, doi: 10.3892/etm.2018.5993.
[103] C. Théry *et al.*, "Minimal information for studies of extracellular vesicles 2018 (MISEV2018): a position statement of the International Society for Extracellular Vesicles and update of the MISEV2014 guidelines," *Journal of Extracellular Vesicles*, vol. 7, no. 1, p. 1535750, 2018, doi: 10.1080/20013078.2018.1535750.
[104] W. M. Henne, N. J. Buchkovich, and S. D. Emr, "The ESCRT Pathway," *Developmental Cell*, vol. 21, no. 1, pp. 77–91, Jul. 2011, doi: 10.1016/j.devcel.2011.05.015.
[105] K. Trajkovic *et al.*, "Ceramide Triggers Budding of Exosome Vesicles into Multivesicular Endosomes," *Science*, vol. 319, no. 5867, pp. 1244–1247, Feb. 2008, doi: 10.1126/science.1153124.
[106] J. Kowal, M. Tkach, and C. Théry, "Biogenesis and secretion of exosomes," *Current Opinion in Cell Biology*, vol. 29, pp. 116–125, Aug. 2014, doi: 10.1016/j.ceb.2014.05.004.
[107] M. Dihné, H.-P. Hartung, and R. J. Seitz, "Restoring Neuronal Function After Stroke by Cell Replacement," *Stroke*, vol. 42, no. 8, pp. 2342–2350, Aug. 2011, doi: 10.1161/STROKEAHA.111.613422.
[108] Y. Li *et al.*, "Human marrow stromal cell therapy for stroke in rat: Neurotrophins and functional recovery," *Neurology*, vol. 59, no. 4, pp. 514–523, Aug. 2002, doi: 10.1212/WNL.59.4.514.
[109] X.-L. Fan, Y. Zhang, X. Li, and Q.-L. Fu, "Mechanisms underlying the protective effects of mesenchymal stem cell-based therapy," *Cell Mol Life Sci*, vol. 77, no. 14, pp. 2771–2794, 2020, doi: 10.1007/s00018-020-03454-6.
[110] I. Smart and C. P. Leblond, "Evidence for division and transformations of neuroglia cells in the mouse brain, as derived from radioautography after injection of thymidine-H3," *Journal of Comparative Neurology*, vol. 116, no. 3, pp. 349–367, 1961, doi: 10.1002/cne.901160307.

[111] J. Altman, “Are new neurons formed in the brains of adult mammals?,” *Science*, vol. 135, no. 3509, pp. 1127–1128, 1962.
[112] J. Altman, “Autoradiographic investigation of cell proliferation in the brains of rats and cats,” *The Anatomical Record*, vol. 145, no. 4, pp. 573–591, 1963, doi: 10.1002/ar.1091450409.
[113] M. S. Kaplan and J. W. Hinds, “Neurogenesis in the adult rat: electron microscopic analysis of light radioautographs,” *Science*, vol. 197, no. 4308, pp. 1092–1094, 1977.
[114] L. Wei, J. L. Fraser, Z.-Y. Lu, X. Hu, and S. P. Yu, “Transplantation of hypoxia preconditioned bone marrow mesenchymal stem cells enhances angiogenesis and neurogenesis after cerebral ischemia in rats,” *Neurobiology of Disease*, vol. 46, no. 3, pp. 635–645, Jun. 2012, doi: 10.1016/j.nbd.2012.03.002.
[115] D. M. Hermann and M. Chopp, “Promoting brain remodelling and plasticity for stroke recovery: therapeutic promise and potential pitfalls of clinical translation,” *The Lancet Neurology*, vol. 11, no. 4, pp. 369–380, Apr. 2012, doi: 10.1016/S1474-4422(12)70039-X.
[116] T. Ozaki, H. Nakamura, and H. Kishima, “Therapeutic strategy against ischemic stroke with the concept of neurovascular unit,” *Neurochemistry International*, vol. 126, pp. 246–251, Jun. 2019, doi: 10.1016/j.neuint.2019.03.022.
[117] G. Qiu *et al.*, “Functional proteins of mesenchymal stem cell-derived extracellular vesicles,” *Stem Cell Res Ther*, vol. 10, no. 1, p. 359, Nov. 2019, doi: 10.1186/s13287-019-1484-6.
[118] P. Gangadaran *et al.*, “Extracellular vesicles from mesenchymal stem cells activates VEGF receptors and accelerates recovery of hindlimb ischemia,” *Journal of Controlled Release*, vol. 264, pp. 112–126, Oct. 2017, doi: 10.1016/j.jconrel.2017.08.022.
[119] H. Gonzalez-King, N. A. García, I. Ontoria-Oviedo, M. Ciria, J. A. Montero, and P. Sepúlveda, “Hypoxia inducible factor-1α potentiates jagged 1-mediated angiogenesis by mesenchymal stem cell-derived exosomes,” *Stem cells*, vol. 35, no. 7, pp. 1747–1759, 2017.
[120] Y. Yang, Y. Cai, Y. Zhang, J. Liu, and Z. Xu, “Exosomes Secreted by Adipose-Derived Stem Cells Contribute to Angiogenesis of Brain Microvascular Endothelial Cells Following Oxygen–Glucose Deprivation In Vitro Through MicroRNA-181b/TRPM7 Axis,” *J Mol Neurosci*, vol. 65, no. 1, pp. 74–83, May 2018, doi: 10.1007/s12031-018-1071-9.
[121] S. Hu *et al.*, “MicroRNA-210 as a Novel Therapy for Treatment of Ischemic Heart Disease,” *Circulation*, vol. 122, no. 11_suppl_1, pp. S124–S131, Sep. 2010, doi: 10.1161/CIRCULATIONAHA.109.928424.
[122] D. R. Cooper *et al.*, “Human adipose-derived stem cell conditioned media and exosomes containing MALAT1 promote human dermal fibroblast migration and ischemic wound healing,” *Advances in wound care*, vol. 7, no. 9, pp. 299–308, 2018.
[123] M. Gong *et al.*, “Mesenchymal stem cells release exosomes that transfer miRNAs to endothelial cells and promote angiogenesis,” *Oncotarget*, vol. 8, no. 28, p. 45200, 2017.
[124] X. Liang, L. Zhang, S. Wang, Q. Han, and R. C. Zhao, “Exosomes secreted by mesenchymal stem cells promote endothelial cell angiogenesis by transferring miR-125a,” *Journal of cell science*, vol. 129, no. 11, pp. 2182–2189, 2016.
[125] O. Rajkovic, G. Potjewyd, and E. Pinteaux, “Regenerative Medicine Therapies for Targeting Neuroinflammation After Stroke,” *Front. Neurol.*, vol. 9, 2018, doi: 10.3389/fneur.2018.00734.
[126] K.-H. Chen *et al.*, “Human induced pluripotent stem cell-derived mesenchymal stem cell therapy effectively reduced brain infarct volume and preserved neurological function in rat

after acute intracranial hemorrhage," *Am J Transl Res*, vol. 11, no. 9, pp. 6232–6248, Sep. 2019.
[127] R. Jin, G. Yang, and G. Li, "Inflammatory mechanisms in ischemic stroke: role of inflammatory cells," *Journal of Leukocyte Biology*, vol. 87, no. 5, pp. 779–789, 2010, doi: 10.1189/jlb.1109766.
[128] G. W. Kreutzberg, "Microglia: a sensor for pathological events in the CNS," *Trends in Neurosciences*, vol. 19, no. 8, pp. 312–318, Aug. 1996, doi: 10.1016/0166-2236(96)10049-7.
[129] S. Dabrowska, A. Andrzejewska, B. Lukomska, and M. Janowski, "Neuroinflammation as a target for treatment of stroke using mesenchymal stem cells and extracellular vesicles," *Journal of Neuroinflammation*, vol. 16, no. 1, p. 178, Sep. 2019, doi: 10.1186/s12974-019-1571-8.
[130] A. Mizuma and M. A. Yenari, "Anti-Inflammatory Targets for the Treatment of Reperfusion Injury in Stroke," *Front. Neurol.*, vol. 8, 2017, doi: 10.3389/fneur.2017.00467.
[131] M. Jiang *et al.*, "Exosomes from MiR-30d-5p-ADSCs Reverse Acute Ischemic Stroke-Induced, Autophagy-Mediated Brain Injury by Promoting M2 Microglial/Macrophage Polarization," *CPB*, vol. 47, no. 2, pp. 864–878, 2018, doi: 10.1159/000490078.
[132] V. Go *et al.*, "Extracellular vesicles from mesenchymal stem cells reduce microglial-mediated neuroinflammation after cortical injury in aged Rhesus monkeys," *GeroScience*, vol. 42, no. 1, pp. 1–17, Feb. 2020, doi: 10.1007/s11357-019-00115-w.
[133] N. J. Abbott, "Inflammatory Mediators and Modulation of Blood–Brain Barrier Permeability," *Cell Mol Neurobiol*, vol. 20, no. 2, pp. 131–147, Apr. 2000, doi: 10.1023/A:1007074420772.
[134] E. Dejonckheere, R. E. Vandenbroucke, and C. Libert, "Matrix metalloproteinases as drug targets in ischemia/reperfusion injury," *Drug Discovery Today*, vol. 16, no. 17, pp. 762–778, Sep. 2011, doi: 10.1016/j.drudis.2011.06.009.
[135] R. L. Jayaraj, S. Azimullah, R. Beiram, F. Y. Jalal, and G. A. Rosenberg, "Neuroinflammation: friend and foe for ischemic stroke," *Journal of Neuroinflammation*, vol. 16, no. 1, p. 142, Jul. 2019, doi: 10.1186/s12974-019-1516-2.
[136] Z. Cheng *et al.*, "Mesenchymal stem cells attenuate blood-brain barrier leakage after cerebral ischemia in mice," *Journal of Neuroinflammation*, vol. 15, no. 1, p. 135, May 2018, doi: 10.1186/s12974-018-1153-1.
[137] M. Chen *et al.*, "The inhibitory effect of mesenchymal stem cell on blood–brain barrier disruption following intracerebral hemorrhage in rats: contribution of TSG-6," *Journal of Neuroinflammation*, vol. 12, no. 1, p. 61, Apr. 2015, doi: 10.1186/s12974-015-0284-x.
[138] A. Kalani *et al.*, "Curcumin-loaded embryonic stem cell exosomes restored neurovascular unit following ischemia-reperfusion injury," *The International Journal of Biochemistry & Cell Biology*, vol. 79, pp. 360–369, Oct. 2016, doi: 10.1016/j.biocel.2016.09.002.
[139] K. Shi, D.-C. Tian, Z.-G. Li, A. F. Ducruet, M. T. Lawton, and F.-D. Shi, "Global brain inflammation in stroke," *The Lancet Neurology*, vol. 18, no. 11, pp. 1058–1066, Nov. 2019, doi: 10.1016/S1474-4422(19)30078-X.
[140] C. Yang, K. E. Hawkins, S. Doré, and E. Candelario-Jalil, "Neuroinflammatory mechanisms of blood-brain barrier damage in ischemic stroke," *American Journal of Physiology-Cell Physiology*, vol. 316, no. 2, pp. C135–C153, Feb. 2019, doi: 10.1152/ajpcell.00136.2018.
[141] C. Iadecola and J. Anrather, "The immunology of stroke: from mechanisms to translation," *Nat Med*, vol. 17, no. 7, Art. no. 7, Jul. 2011, doi: 10.1038/nm.2399.

[142] Y. Feng *et al.*, "Infiltration and persistence of lymphocytes during late-stage cerebral ischemia in middle cerebral artery occlusion and photothrombotic stroke models," *J Neuroinflammation*, vol. 14, no. 1, p. 248, Dec. 2017, doi: 10.1186/s12974-017-1017-0.
[143] M. Campanella, C. Sciorati, G. Tarozzo, and M. Beltramo, "Flow Cytometric Analysis of Inflammatory Cells in Ischemic Rat Brain," *Stroke*, vol. 33, no. 2, pp. 586–592, Feb. 2002, doi: 10.1161/hs0202.103399.
[144] M. L. Shiao *et al.*, "Immunomodulation with Human Umbilical Cord Blood Stem Cells Ameliorates Ischemic Brain Injury – A Brain Transcriptome Profiling Analysis," *Cell Transplant*, vol. 28, no. 7, pp. 864–873, Jul. 2019, doi: 10.1177/0963689719836763.
[145] R. L. Webb *et al.*, "Human Neural Stem Cell Extracellular Vesicles Improve Recovery in a Porcine Model of Ischemic Stroke," *Stroke*, vol. 49, no. 5, pp. 1248–1256, May 2018, doi: 10.1161/STROKEAHA.117.020353.
[146] S. Dabrowska, A. Andrzejewska, D. Strzemecki, M. Muraca, M. Janowski, and B. Lukomska, "Human bone marrow mesenchymal stem cell-derived extracellular vesicles attenuate neuroinflammation evoked by focal brain injury in rats," *J Neuroinflammation*, vol. 16, no. 1, p. 216, Nov. 2019, doi: 10.1186/s12974-019-1602-5.
[147] B. S. Bhatnagar, R. H. Bogner, and M. J. Pikal, "Protein stability during freezing: separation of stresses and mechanisms of protein stabilization," *Pharm Dev Technol*, vol. 12, no. 5, pp. 505–523, 2007, doi: 10.1080/10837450701481157.
[148] P. L. Privalov, "Cold denaturation of protein," *Critical reviews in biochemistry and molecular biology*, vol. 25, no. 4, pp. 281–306, 1990.
[149] R. Jaenicke, "Protein structure and function at low temperatures," *Philosophical Transactions of the Royal Society of London. B, Biological Sciences*, vol. 326, no. 1237, pp. 535–553, 1990.
[150] F. Franks and R. H. Hatley, "Stability of proteins at subzero temperatures: thermodynamics and some ecological consequences," *Pure and applied chemistry*, vol. 63, no. 10, pp. 1367–1380, 1991.
[151] M. J. Pikal, "Mechanisms of Protein Stabilization During Freeze-Drying Storage: The Relative Importance of Thermodynamic Stabilization and Glassy State Relaxation Dynamics," in *Freeze-Drying/Lyophilization of Pharmaceutical and Biological Products*, 3rd ed., CRC Press, 2010.
[152] R. E. Pincock, "Reactions in frozen systems," *Accounts of Chemical Research*, vol. 2, no. 4, pp. 97–103, 1969.
[153] R. Parker and S. Ring, "A theoretical analysis of diffusion-controlled reactions in frozen solutions," *Cryo-Letters*, vol. 16, no. 4, pp. 197–208, 1995.
[154] T. C. BRUICE and A. R. BUTLER, "Ionic reactions in frozen aqueous systems," presented at the Federation proceedings, 1965, vol. 24, pp. S45–S49.
[155] R. H. Hatley, F. Franks, and H. Day, "Subzero-temperature preservation of reactive fluids in the undercooled state: II. The effect on the oxidation of ascorbic acid of freeze concentration and undercooling," *Biophysical chemistry*, vol. 24, no. 2, pp. 187–192, 1986.
[156] D. Champion, G. Blond, M. Le Meste, and D. Simatos, "Reaction rate modeling in cryoconcentrated solutions: Alkaline phosphatase catalyzed DNPP hydrolysis," *Journal of agricultural and food chemistry*, vol. 48, no. 10, pp. 4942–4947, 2000.
[157] N. S. Terefe, J. M. Arimi, A. Van Loey, and M. Hendrickx, "Kinetics of the Alkaline Phosphatase Catalyzed Hydrolysis of Disodium p-Nitrophenyl Phosphate: Effects of

Carbohydrate Additives, Low Temperature, and Freezing," *Biotechnology progress*, vol. 20, no. 5, pp. 1467–1478, 2004.
[158] G. Gómez, M. J. Pikal, and N. Rodríguez-Hornedo, "Effect of initial buffer composition on pH changes during far-from-equilibrium freezing of sodium phosphate buffer solutions," *Pharmaceutical research*, vol. 18, no. 1, pp. 90–97, 2001.
[159] S. Larsen, "Stability of drugs in frozen-systems. VI. Effects of freezing upon pH for buffered aqueous solutions," *J. Biochem*, vol. 81, pp. 163–168, 1973.
[160] N. Murase and F. Franks, "Salt precipitation during the freeze-concentration of phosphate buffer solutions," *Biophysical chemistry*, vol. 34, no. 3, pp. 293–300, 1989.
[161] B. A. Szkudlarek, *Selective crystallization of phosphate buffer components andpH changes during freezing: Implications to protein stability*. University of Michigan, 1997.
[162] Y. Cheng, Q. Zeng, Q. Han, and W. Xia, "Effect of pH, temperature and freezing-thawing on quantity changes and cellular uptake of exosomes," *Protein & Cell*, vol. 10, no. 4, pp. 295–299, 2019.
[163] E. Y. Shalaev, T. D. Johnson-Elton, L. Chang, and M. J. Pikal, "Thermophysical properties of pharmaceutically compatible buffers at sub-zero temperatures: implications for freeze-drying," *Pharmaceutical research*, vol. 19, no. 2, pp. 195–201, 2002.
[164] E. Shalaev, "The impact of buffer on processing and stability of freeze-dried dosage forms, part 1: solution freezing behavior," *American Pharmaceutical Review*, vol. 8, no. 5, p. 80, 2005.
[165] J. Dong, A. Hubel, J. C. Bischof, and A. Aksan, "Freezing-induced phase separation and spatial microheterogeneity in protein solutions," *The Journal of Physical Chemistry B*, vol. 113, no. 30, pp. 10081–10087, 2009.
[166] M. C. Heller, J. F. Carpenter, and T. W. Randolph, "Effects of phase separating systems on lyophilized hemoglobin," *Journal of pharmaceutical sciences*, vol. 85, no. 12, pp. 1358–1362, 1996.
[167] L.-M. Her, M. Deras, and S. L. Nail, "Electrolyte-induced changes in glass transition temperatures of freeze-concentrated solutes," *Pharmaceutical research*, vol. 12, no. 5, pp. 768–772, 1995.
[168] V. Y. Grinberg and V. Tolstoguzov, "Thermodynamic incompatibility of proteins and polysaccharides in solutions," *Food Hydrocolloids*, vol. 11, no. 2, pp. 145–158, 1997.
[169] M. C. Heller, J. F. Carpenter, and T. W. Randolph, "Protein formulation and lyophilization cycle design: Prevention of damage due to freeze-concentration induced phase separation," *Biotechnology and Bioengineering*, vol. 63, no. 2, pp. 166–174, 1999.
[170] Y. Uda, S. Zepeda, F. Kaneko, Y. Matsuura, and Y. Furukawa, "Adsorption-induced conformational changes of antifreeze glycoproteins at the ice/water interface," *The Journal of Physical Chemistry B*, vol. 111, no. 51, pp. 14355–14361, 2007.
[171] F. Susa, G. Bucca, T. Limongi, V. Cauda, and R. Pisano, "Enhancing the preservation of liposomes: The role of cryoprotectants, lipid formulations and freezing approaches," *Cryobiology*, vol. 98, pp. 46–56, 2021.
[172] S. Shukla, "Freeze drying process: A review," *International journal of pharmaceutical sciences and research*, vol. 2, no. 12, p. 3061, 2011.
[173] X. C. Tang and M. J. Pikal, "Design of freeze-drying processes for pharmaceuticals: practical advice," *Pharmaceutical research*, vol. 21, no. 2, pp. 191–200, 2004.
[174] F. K. Bedu-Addo, "Understanding lyophilization formulation development," *Pharmaceutical Technology*, vol. 20, pp. 10–19, 2004.

[175] M. Pikal, S. Shah, M. Roy, and R. Putman, "The secondary drying stage of freeze drying: drying kinetics as a function of temperature and chamber pressure," *International journal of pharmaceutics*, vol. 60, no. 3, pp. 203–207, 1990.
[176] C. Chen, D. Han, C. Cai, and X. Tang, "An overview of liposome lyophilization and its future potential," *Journal of Controlled Release*, vol. 142, no. 3, pp. 299–311, Mar. 2010, doi: 10.1016/j.jconrel.2009.10.024.
[177] A. R. Mohammed, A. G. Coombes, and Y. Perrie, "Amino acids as cryoprotectants for liposomal delivery systems," *European journal of pharmaceutical sciences*, vol. 30, no. 5, pp. 406–413, 2007.
[178] I. I. Katkov and F. Levine, "Prediction of the glass transition temperature of water solutions: comparison of different models," *Cryobiology*, vol. 49, no. 1, pp. 62–82, 2004.
[179] D. Greiff, "Protein structure and freeze-drying: the effects of residual moisture and gases," *Cryobiology*, vol. 8, no. 2, pp. 145–152, 1971.
[180] M. J. Pikal and S. Shah, "Intravial distribution of moisture during the secondary drying stage of freeze drying," *PDA journal of pharmaceutical science and technology*, vol. 51, no. 1, pp. 17–24, 1997.
[181] J. K. Towns, "Moisture content in proteins: its effects and measurement," *Journal of Chromatography A*, vol. 705, no. 1, pp. 115–127, 1995.
[182] D. Kahne and W. C. Still, "Hydrolysis of a peptide bond in neutral water," *Journal of the American Chemical Society*, vol. 110, no. 22, pp. 7529–7534, 1988.
[183] J. A. Rupley and G. Careri, "Protein hydration and function," *Advances in protein chemistry*, vol. 41, pp. 37–172, 1991.
[184] H. Nagendra, N. Sukumar, and M. Vijayan, "Role of water in plasticity, stability, and action of proteins: the crystal structures of lysozyme at very low levels of hydration," *Proteins: Structure, Function, and Bioinformatics*, vol. 32, no. 2, pp. 229–240, 1998.
[185] B. A. Kerwin and R. L. Remmele, "Protect from Light: Photodegradation and Protein Biologics," *Journal of Pharmaceutical Sciences*, vol. 96, no. 6, pp. 1468–1479, Jun. 2007, doi: 10.1002/jps.20815.
[186] W. Vogt, "Oxidation of methionyl residues in proteins: tools, targets, and reversal," *Free Radical Biology and Medicine*, vol. 18, no. 1, pp. 93–105, 1995.
[187] M. J. Davies and R. J. Truscott, "Photo-oxidation of proteins and its role in cataractogenesis," *Journal of Photochemistry and Photobiology B: Biology*, vol. 63, no. 1–3, pp. 114–125, 2001.
[188] L. I. Grossweiner, "Photochemistry of proteins: a review," *Current eye research*, vol. 3, no. 1, pp. 137–144, 1984.
[189] G. Laustriat and C. Hasselmann, "Photochemistry of proteins," *Photochemistry and Photobiology*, vol. 22, no. 6, pp. 295–298, 1975.
[190] L. M. Crowe, J. H. Crowe, A. Rudolph, C. Womersley, and L. Appel, "Preservation of freeze-dried liposomes by trehalose," *Archives of biochemistry and biophysics*, vol. 242, no. 1, pp. 240–247, 1985.
[191] L. M. Crowe and J. H. Crowe, "Hydration-dependent hexagonal phase lipid in a biological membrane," *Archives of biochemistry and biophysics*, vol. 217, no. 2, pp. 582–587, 1982.
[192] P. Kumar and K. L. Mittal, *Handbook of microemulsion science and technology*. Marcel Dekker New York, 1999.
[193] J. W. Goodby *et al.*, "Thermotropic liquid crystalline glycolipids," *Chemical Society Reviews*, vol. 36, no. 12, pp. 1971–2032, 2007.

[194] M. Z. Ashraf and S. Srivastava, "Oxidized phospholipids: introduction and biological significance," in *Lipoproteins-Role in Health and Diseases*, IntechOpen, 2012.
[195] A. Misra, K. Jinturkar, D. Patel, J. Lalani, and M. Chougule, "Recent advances in liposomal dry powder formulations: preparation and evaluation," *Expert opinion on drug delivery*, vol. 6, no. 1, pp. 71–89, 2009.
[196] K. Madin and J. H. Crowe, "Anhydrobiosis in nematodes: carbohydrate and lipid metabolism during dehydration," *Journal of Experimental Zoology*, vol. 193, no. 3, pp. 335–342, 1975.
[197] K. L. Koster and A. C. Leopold, "Sugars and desiccation tolerance in seeds," *Plant physiology*, vol. 88, no. 3, pp. 829–832, 1988.
[198] F. Hoekstra, L. Crowe, and J. Crowe, "Differential desiccation sensitivity of corn and Pennisetum pollen linked to their sucrose contents," *Plant, Cell & Environment*, vol. 12, no. 1, pp. 83–91, 1989.
[199] G. Bianchi, A. Gamba, C. Murelli, F. Salamini, and D. Bartels, "Novel carbohydrate metabolism in the resurrection plant Craterostigma plantagineum," *The Plant journal: for cell and molecular biology*, vol. 1, no. 3, pp. 355–359, 1991.
[200] C. L. Paiva and A. D. Panek, "Biotechnological applications of the disaccharide trehalose," *Biotechnology annual review*, vol. 2, pp. 293–314, 1996.
[201] B. J. Aldous, A. D. Auffret, and F. Franks, "The crystallisation of hydrates from amorphous carbohydrates (Accepted 10th May, 1995)," *Cryo-letters*, vol. 16, no. 3, pp. 181–186, 1995.
[202] H. Levine, "Another view of trehalose for drying and stabilizing biological materials," *BioPharm*, pp. 36–40, 1992.
[203] J. H. Crowe, J. F. Carpenter, L. M. Crowe, and T. J. Anchordoguy, "Are freezing and dehydration similar stress vectors? A comparison of modes of interaction of stabilizing solutes with biomolecules," *Cryobiology*, vol. 27, no. 3, pp. 219–231, 1990.
[204] G. I. Olgenblum, L. Sapir, and D. Harries, "Properties of aqueous trehalose mixtures: glass transition and hydrogen bonding," *Journal of chemical theory and computation*, vol. 16, no. 2, pp. 1249–1262, 2020.
[205] P. F. Fox, *Advanced dairy chemistry volume 3: lactose, water, salts and vitamins*. Springer Science & Business Media, 2013.
[206] K. Roe and T. Labuza, "Glass transition and crystallization of amorphous trehalose-sucrose mixtures," *International journal of food properties*, vol. 8, no. 3, pp. 559–574, 2005.
[207] L. M. Crowe, D. S. Reid, and J. H. Crowe, "Is trehalose special for preserving dry biomaterials?," *Biophysical journal*, vol. 71, no. 4, pp. 2087–2093, 1996.
[208] D. Z. Icoz, C. I. Moraru, and J. L. Kokini, "Polymer–polymer interactions in dextran systems using thermal analysis," *Carbohydrate polymers*, vol. 62, no. 2, pp. 120–129, 2005.
[209] J. H. Crowe, J. F. Carpenter, and L. M. Crowe, "The role of vitrification in anhydrobiosis," *Annual review of physiology*, vol. 60, no. 1, pp. 73–103, 1998.
[210] A. Patist and H. Zoerb, "Preservation mechanisms of trehalose in food and biosystems," *Colloids and Surfaces B: Biointerfaces*, vol. 40, no. 2, pp. 107–113, 2005.
[211] J. H. Crowe, L. M. Crowe, and S. A. Jackson, "Preservation of structural and functional activity in lyophilized sarcoplasmic reticulum," *Archives of Biochemistry and Biophysics*, vol. 220, no. 2, pp. 477–484, 1983.
[212] S. Magazù, V. Villari, P. Migliardo, G. Maisano, and M. Telling, "Diffusive dynamics of water in the presence of homologous disaccharides: A comparative study by quasi elastic

neutron scattering. IV.," *The Journal of Physical Chemistry B*, vol. 105, no. 9, pp. 1851–1855, 2001.
[213] A. D. Elbein, Y. Pan, I. Pastuszak, and D. Carroll, "New insights on trehalose: a multifunctional molecule," *Glycobiology*, vol. 13, no. 4, pp. 17R-27R, 2003.
[214] S. Stewart and X. He, "Intracellular delivery of trehalose for cell banking," *Langmuir*, vol. 35, no. 23, pp. 7414–7422, 2018.
[215] K. Takeuchi, M. Nakazawa, and Y. Ebina, "Effects of trehalose on VEGF-stimulated angiogenesis and myofibroblast proliferation: implications for glaucoma filtration surgery," *Investigative Ophthalmology & Visual Science*, vol. 52, no. 9, pp. 6987–6993, 2011.
[216] C. Charoenviriyakul, Y. Takahashi, M. Nishikawa, and Y. Takakura, "Preservation of exosomes at room temperature using lyophilization," *International Journal of Pharmaceutics*, vol. 553, no. 1, pp. 1–7, Dec. 2018, doi: 10.1016/j.ijpharm.2018.10.032.
[217] H.-J. Lee, Y.-S. Yoon, and S.-J. Lee, "Mechanism of neuroprotection by trehalose: controversy surrounding autophagy induction," *Cell Death Dis*, vol. 9, no. 7, p. 712, Jun. 2018, doi: 10.1038/s41419-018-0749-9.
[218] C. De Duve, B. Pressman, R. Gianetto, R. Wattiaux, and F. Appelmans, "Tissue fractionation studies. 6. Intracellular distribution patterns of enzymes in rat-liver tissue," *Biochemical Journal*, vol. 60, no. 4, p. 604, 1955.
[219] M. Casarejos, R. Solano, A. Gomez, J. Perucho, J. De Yébenes, and M. Mena, "The accumulation of neurotoxic proteins, induced by proteasome inhibition, is reverted by trehalose, an enhancer of autophagy, in human neuroblastoma cells," *Neurochemistry international*, vol. 58, no. 4, pp. 512–520, 2011.
[220] S. Sarkar *et al.*, "Neuroprotective effect of the chemical chaperone, trehalose in a chronic MPTP-induced Parkinson's disease mouse model," *Neurotoxicology*, vol. 44, pp. 250–262, 2014.
[221] M. Tanaka *et al.*, "Trehalose alleviates polyglutamine-mediated pathology in a mouse model of Huntington disease," *Nature Medicine*, vol. 10, no. 2, Art. no. 2, Feb. 2004, doi: 10.1038/nm985.
[222] A. Munshi *et al.*, "A comprehensive proteomics profiling identifies NRP1 as a novel identity marker of human bone marrow mesenchymal stromal cell-derived small extracellular vesicles," *Stem Cell Research & Therapy*, vol. 10, no. 1, p. 401, Dec. 2019, doi: 10.1186/s13287-019-1516-2.
[223] K. L. DeCicco-Skinner *et al.*, "Endothelial Cell Tube Formation Assay for the In Vitro Study of Angiogenesis," *JoVE (Journal of Visualized Experiments)*, no. 91, p. e51312, Sep. 2014, doi: 10.3791/51312.

8 Appendix

8.1 MicroBCA assay protocol

1. According to Table 1 albumin standards were prepared following a serial dilution procedure.

Table 1. Preparation of albumin standards.

Standard identifier	Volume of PBS (mL)	Volume of source albumin (mL)	Final Albumin concentration (µg/mL)
A	4.5	0.5 from stock	200
B	8.0	2.0 from vial A	40
C	4.0	4.0 from vial B	20
D	4.0	4.0 from vial C	10
E	4.0	4.0 from vial D	5
F	4.0	4.0 from vial E	2.5
G	4.8	3.2 from vial F	1
H	4.0	4.0 from vial G	0.5
I	8.0	0	0

2. Working reagent was then prepared by mixing 25-parts of microBCA reagent MA with 24-parts reagent MB and 1-part reagent MC. For instance, to produce 10 mL of working reagent, blend 5 mL of reagent MA, 4.8 mL of reagent MB, and 0.2 mL of reagent MC.
3. Then pipette 150 µL of MSC-EV sample or standard (in replicates) into the wells of a 96-well plate.
4. Add 150 µL of working reagent to the wells and place on shaker for 30 seconds.
5. The plate was then incubated at 37^{o}C for 2 hours and the absorbance was measured at 562 nm
6. The blank absorbance was then subtracted from all other standards and samples
7. A standard curve was then developed following a polynomial regression and the protein concentration of the MSC-EVs was determined.